Quaternary Science Reviews xxx (2015) 1–16

Contents lists available at ScienceDirect

Quaternary Science Reviews

journal homepage: www.elsevier.com/locate/quascirev

Holocene sea subsurface and surface water masses in the Fram Strait – Comparisons of temperature and sea-ice reconstructions

Kirstin Werner [a, *], Juliane Müller [b], Katrine Husum [c], Robert F. Spielhagen [d, e], Evgenia S. Kandiano [e], Leonid Polyak [a]

[a] Byrd Polar and Climate Research Center, The Ohio State University, 1090 Carmack Road, Columbus OH-43210, USA
[b] Alfred Wegener Institute, Helmholtz Centre for Polar and Marine Research, Am Alten Hafen 26, 27568 Bremerhaven, Germany
[c] Norwegian Polar Institute, Framsenteret, Hjalmar Johansens Gate 14, 9296 Tromsø, Norway
[d] Academy of Sciences, Humanities, and Literature Mainz, Geschwister-Scholl-Straße 2, 55131 Mainz, Germany
[e] GEOMAR Helmholtz Centre for Ocean Research, Wischhofstr. 1-3, 24148 Kiel, Germany

ARTICLE INFO

Article history:
Received 30 April 2015
Received in revised form
19 August 2015
Accepted 1 September 2015
Available online xxx

Keywords:
Fram strait
Holocene
Sea surface temperatures
Subsurface
Sea ice
Atlantic water
Planktic foraminifera
Biomarkers
IP25

ABSTRACT

Two high-resolution sediment cores from eastern Fram Strait have been investigated for sea subsurface and surface temperature variability during the Holocene (the past ca 12,000 years). The transfer function developed by Husum and Hald (2012) has been applied to sediment cores in order to reconstruct fluctuations of sea subsurface temperatures throughout the period. Additional biomarker and foraminiferal proxy data are used to elucidate variability between surface and subsurface water mass conditions, and to conclude on the Holocene climate and oceanographic variability on the West Spitsbergen continental margin. Results consistently reveal warm sea surface to subsurface temperatures of up to 6 °C until ca 5 cal ka BP, with maximum seawater temperatures around 10 cal ka BP, likely related to maximum July insolation occurring at that time. Maximum Atlantic Water (AW) advection occurred at surface and subsurface between 10.6 and 8.5 cal ka BP based on both foraminiferal and dinocyst temperature reconstructions. Probably, a less-stratified, ice-free, nutrient-rich surface ocean with strong AW advection prevailed in the eastern Fram Strait between 10 and 9 cal ka BP. Weakened AW contribution is found after ca 5 cal ka BP when subsurface temperatures strongly decrease with minimum values between ca 4 and 3 cal ka BP. Cold late Holocene conditions are furthermore supported by high planktic foraminifer shell fragmentation and high $\delta^{18}O$ values of the subpolar planktic foraminifer species *Turborotalita quinqueloba*. While IP_{25}-associated indices as well as dinocyst data suggest a sustained cooling due to a decrease in early summer insolation and consequently sea-ice increase since about 7 cal ka BP in surface waters, planktic foraminiferal data including stable isotopes indicate a slight return of stronger subsurface AW influx since ca 3 cal ka BP. The observed decoupling of surface and subsurface waters during the later Holocene is most likely attributed to a strong pycnocline layer separating cold sea-ice fed surface waters from enhanced subsurface AW advection. This may be related to changes in North Atlantic subpolar versus subtropical gyre activity.

1. Introduction

In the Arctic, effects of global climate change occur more rapidly and severe than in other regions on Earth due to the polar amplification (Manabe and Stouffer, 1980). Over the past few decades, the Arctic sea-ice cover has been shrinking continuously while more heat is delivered to the high north through different atmospheric and oceanic mechanisms. Climate model projections not only predict a change from perennial to more seasonal sea-ice cover in the Arctic but also globally rising sea level with significant feedbacks to global climate (e.g., Bengtsson et al., 2006).

The Fram Strait between Greenland and Svalbard is the only deepwater connection where warm and cold surface to deep water masses exchange between the Arctic and the world's oceans. Northward flowing warm and saline Atlantic Water (AW) via the eastern Fram Strait strongly contributes to the Arctic Ocean's heat budget.

Reconstructions of past climate and oceanographic conditions

* Corresponding author.
E-mail address: werner.192@osu.edu (K. Werner).

http://dx.doi.org/10.1016/j.quascirev.2015.09.007
0277-3791/

are essential for understanding and modelling of the current and future climate. Extending the record of ocean temperatures beyond the era of instrumental measurements facilitates improved knowledge about the long-term mechanisms of heat advection into the Arctic Ocean and water mass stratification. This also includes their forcing factors such as insolation, sea-ice extent, ocean current strength, and sea-level changes. During recent decades, the eastern Fram Strait as the major gateway between the northern North Atlantic and the Arctic Ocean has been studied extensively to better understand Holocene environmental changes (Hald et al., 2004; 2007; Ślubowska et al., 2005; Rasmussen et al., 2007, 2013; Ślubowska-Woldengen et al., 2008; Müller et al., 2009; 2011; 2012; Werner et al., 2011; 2013; 2014; Aagaard-Sørensen et al., 2014a,b) However, complex water mass interactions complicate straightforward reconstructions of past water mass temperatures in the area. In this paper, Holocene planktic foraminifera from the eastern Fram Strait have been used to reconstruct past sea subsurface water temperatures using transfer functions (Husum and Hald, 2012). Modern planktic foraminifer assemblages are dominated by two main species *Neogloboquadrina pachyderma* and *Turborotalita quinqueloba*. *N. pachyderma* is associated with cold polar waters (e.g., Bé and Tolderlund, 1971; Volkmann, 2000) while *T. quinqueloba* is commonly linked to warm and saline Atlantic Water advection in the Fram Strait area (Volkmann, 2000), in addition to the Arctic Front where Atlantic and Arctic water masses encounter (Johannessen et al., 1994; Matthiessen et al., 2001). *T. quinqueloba* is a symbiont-bearing foraminifer that is therefore bound to the uppermost photic zone due to required light conditions for photosynthetic activity (Bé, 1977). Different from studies in the central Irminger Sea where both species record temperatures around the same depth but during different periods of the spring/summer season (Jonkers et al., 2010), recent studies of living planktic foraminifera from the Fram Strait show no clear differences in seasonal flux patterns between *N. pachyderma* and *T. quinqueloba.* Depending on water mass and sea-ice conditions, both species inhabit rather similar summer depth habitats within the uppermost ca 200 m of the water column (Manno and Pavlov, 2014; Pados and Spielhagen, 2014). Previous studies from the Fram Strait and western Svalbard have shown heat advection to the Arctic Ocean was enhanced during the Early Holocene, driven by maximum summer insolation and wind force and/or thermohaline circulation (e.g., Koç et al., 1993; Hald et al., 2007; Rasmussen et al., 2007; 2013; Ślubowska-Woldengen et al., 2008). Most studies indicate a cooling trend after ca 8 cal ka BP (Hald et al., 2004; Ślubowska-Woldengen et al., 2007; Müller et al., 2012). A significantly warmer Mid-Holocene and probably increased heat flux to the Arctic Ocean was found by some studies in the Barents Sea/Svalbard area with ocean temperatures likely higher than for the remainder of the Holocene (e.g., Sarnthein et al., 2003; Hald et al., 2007; Rasmussen et al., 2007). Consistent with a decreasing summer insolation during the late Holocene, compared to the preceding early and mid-Holocene intervals, reconstructed seawater temperatures were lower; and more stable conditions with extended sea-ice conditions prevailed in the area (Sarnthein et al., 2003; Müller et al., 2012; Werner et al., 2013). However, many of the reconstructions using planktic foraminifera and transfer functions were based on transfer functions with only few polar and subpolar modern analogues (e.g., Kucera et al., 2005; Husum and Hald, 2012).

Two high-resolution sediment cores comprising the last ca 12,000 years have been studied for planktic foraminiferal content in order to reconstruct sea subsurface temperatures at 100 m water depth (SST100; cf. Husum and Hald, 2012). Proxy data such as the ice-rafted debris and biomarkers complement SST100 reconstructions for a comprehensive reconstruction of Holocene variability in this crucial area with regards to the changing modern Arctic system. The spring sea ice proxy IP_{25} (Belt et al., 2007; Brown et al., 2014), the ratio of IP_{25} to its structurally related C_{25} highly branched isoprenoid (C_{25}-HBI)diene (DIP_{25} index; Fahl and Stein, 2012; Cabedo-Sanz et al., 2013), and biomarkers indicative of phytoplankton productivity allow estimates of sea-ice and primary-productivity changes associated with temperature variations at the core site. Previously, it has been assumed that the DIP_{25} index could refer to relative sea surface temperature (at ca 10 m water depth; SST10) changes (Xiao et al., 2013; Müller and Stein, 2014). Here, for the first time, DIP_{25} values are directly compared to reconstructed ocean temperature trends, which may give insight into the suitability of the DIP_{25} index as a potential SST10 proxy.

2. Hydrography

Northward flowing warm and saline Atlantic Water enters the Arctic Ocean as the West Spitsbergen Current (WSC) via the eastern Fram Strait (Fig. 1). The WSC delivers warm and saline (T up to 6 °C, S > 35, Figs. 1 and 2) AW at surface to subsurface water depths to the Arctic Ocean where its upper part becomes transformed into a less saline surface layer by ice melt and mixing with low-saline waters of mainly riverine origin.

The strength of northward flowing AW is affected by the variability of both the cyclonic subpolar gyre (SPG) and the anticyclonic subtropical gyre (STG) in the North Atlantic Ocean (Hátún et al., 2005). In particular, increasing salinities in the northeastern part of the North Atlantic have been found to correspond to decreasing circulation of the SPG (Häkkinen and Rhines, 2004) as well as to the shape of the gyre (Hátún et al., 2005).

In response to Arctic Ocean surface current patterns (Transpolar Drift and Beaufort gyre), sea ice as well as cold, fresh water masses exit along western Fram Strait as part of the East Greenland Current (EGC), which carries cold and fresh polar waters (T < 0 °C, S < 34.4; e.g., Rabe et al., 2009) towards the Greenland Sea. Accordingly, sea-ice extent in the Fram Strait is controlled by two opposite current systems keeping eastern Fram Strait at present ice-free year-round while western Fram Strait stays perennially sea-ice covered.

3. Material and methods

The 9.54 m long Kastenlot core MSM5/5-723-2 from the eastern Fram Strait (79°9′N, 5°20′E, 1350 m water depth) was retrieved in summer 2007 during cruise leg MSM5/5 with RV Maria S. Merian. The uppermost section of the sediment core (4.75 m) was investigated at high resolution for proxy climate indicators such as biomarkers, foraminiferal assemblages and stable isotopes, and contents of ice-rafted debris. The studied section consists of dark olive to brownish black silty clays where from visual core inspection no evidence for abrupt changes in sedimentation rates such as hiatuses etc. could be indicated. Age control of the sediment core is based on six accelerator mass spectrometry (AMS) radiocarbon dates which had been published previously by Müller et al. (2012). To the existing age-depth-model we add two more dates (Table 1; Fig. 3). Analyses were conducted at the Leibniz Laboratory of Kiel University using ca 10 mg of $CaCO_3$. All measurements were carried out on a single species *N. pachyderma*. Radiocarbon dates were converted to calendar years BP (present = 1950 AD) applying the calibration software Calib version 7.1 (Stuiver and Reimer, 1993) with the Marine13 calibration data set (Reimer et al., 2009), including a reservoir correction of ~400 years. Chronology is established using the calibrated calendar ages and assuming uniform sedimentation rates between them by linear interpolation.

Please cite this article in press as: Werner, K., et al., Holocene sea subsurface and surface water masses in the Fram Strait – Comparisons of temperature and sea-ice reconstructions, Quaternary Science Reviews (2015), http://dx.doi.org/10.1016/j.quascirev.2015.09.007

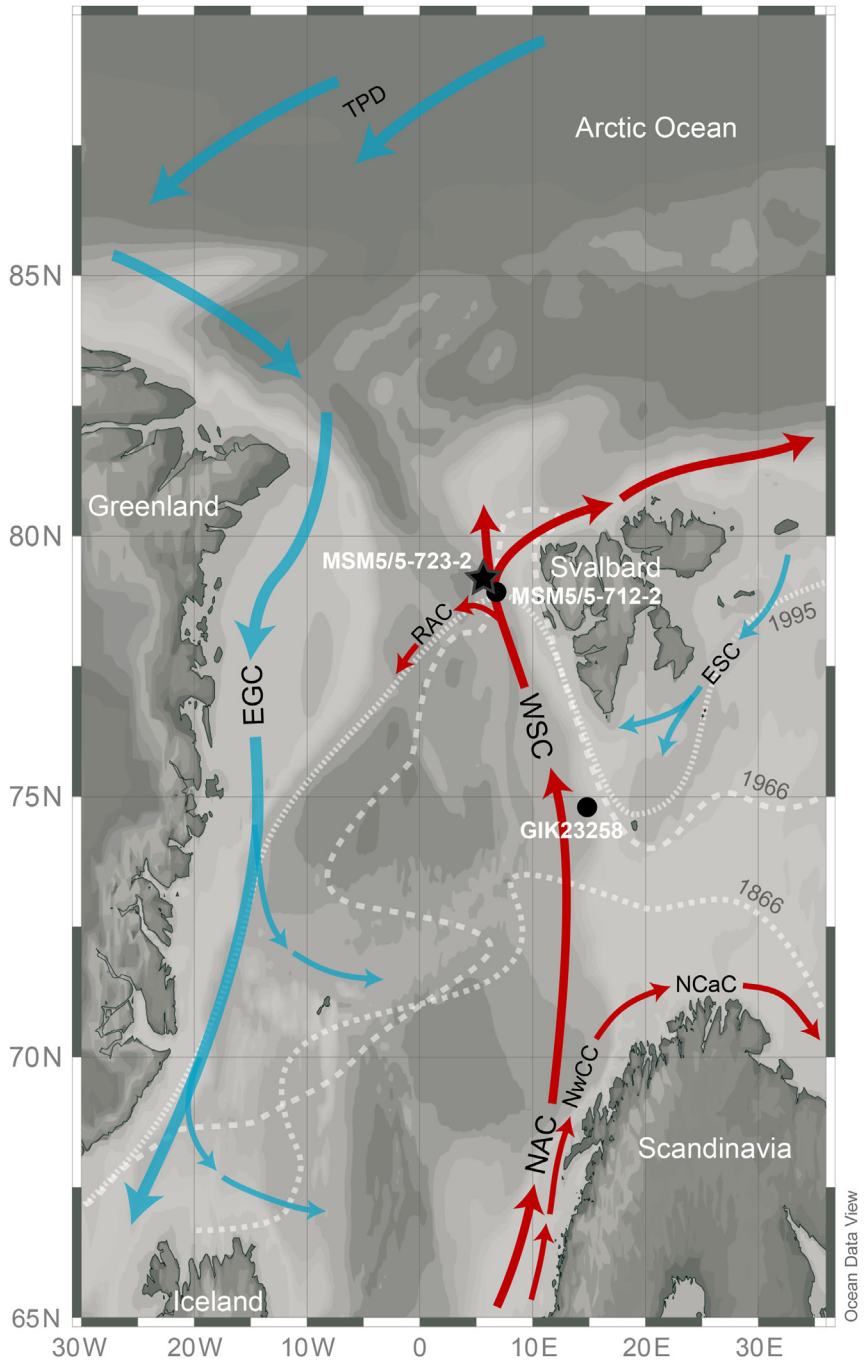

Fig. 1. Map of the study area showing the investigated core location MSM5/5-723-2 (asterisk) as well as other sediment cores mentioned in the text (filled circles). Warm and saline Atlantic Water advection and cold polar surface waters of Arctic origin are indicated by red and blue arrows, respectively. The dashed lines show approximate recent locations of the maximum sea-ice margins after Vinje (2001). EGC East Greenland Current, ESC East Spitsbergen Current, NAC North Atlantic Current, NCaC North Cape Current, NwCC Norwegian Coastal Current, RAC Return Atlantic Current, TPD Transpolar Drift, WSC West Spitsbergen Current. (For interpretation of the references to colour in this figure legend, the reader is referred to the web version of this article.).

In addition, previously published results of sediment core MSM5/5-712-2 from the eastern Fram Strait (Müller et al., 2012; Werner et al., 2013; Aagaard-Sørensen et al., 2014a) will be discussed and complement the new SST100 reconstruction.

3.1. Foraminiferal-derived climate proxy indicators

Sediment samples were freeze-dried, and dry bulk density was determined from defined 10 cm^3 samples at 10–20 cm intervals. From samples washed through a 63 μm sieve prior to analysis, a representative split of at least 300 planktic foraminifer specimens was counted in size fraction 100–250 μm and identified to species level in order to apply the Husum and Hald (2012) transfer function and derive sea subsurface temperatures for the past 12,000 years (see 3.2).

In addition, fragmentation of planktic foraminifer tests has been monitored in size fraction 100–250 μm by counting planktic foraminifer test fragments that were no more determinable to species

Please cite this article in press as: Werner, K., et al., Holocene sea subsurface and surface water masses in the Fram Strait – Comparisons of temperature and sea-ice reconstructions, Quaternary Science Reviews (2015), http://dx.doi.org/10.1016/j.quascirev.2015.09.007

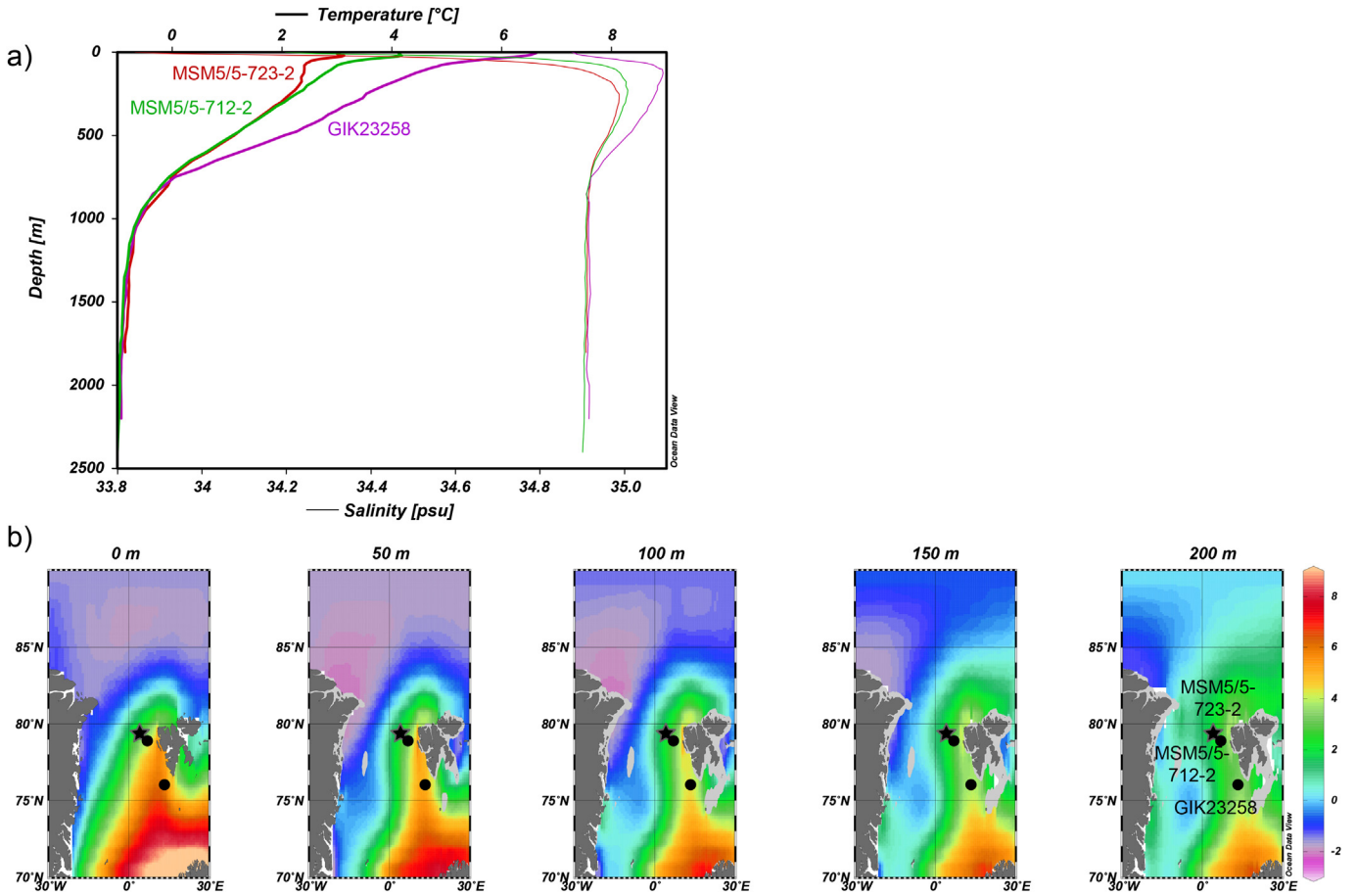

Fig. 2. a) Water mass profiles (July to September, 1955 to 2012) from locations close to the sediment cores shown in Fig. 1. b) Surface to subsurface temperatures at 0, 50, 100, 150, and 200 m water depths in the study area (July to September, 1955 to 2012). The current core location is indicated with an asterisk and others mentioned in the text with a filled circle. All data compiled from WOA13 and ODV.

Table 1
AMS radiocarbon dates and calibrated dates for kastenlot core MSM5/5-723-2 (see also Müller et al., 2012). All datings were carried out on tests of the planktic foraminifer species *N. pachyderma*.

Depth, cm	^{14}C age, yr	Cal. age, yr BP (2σ)	Lab. No
10.0–13.0[a]	675.5 ± 25	335.5 ± 68.5	KIA 38738
50.0–53.0[a]	2125 ± 25	1708.5 ± 92.5	KIA 38700
102.0–103.0[a]	3820 ± 30	3769.5 ± 99.5	KIA 43851
130.0–133.0[a]	4950 ± 35	5317 ± 118	KIA 38739
180.0–182.0[a]	6120 ± 40	6545.5 ± 107.5	KIA 43852
230.0–233.0[a]	7290 ± 40	7752.5 ± 96.5	KIA 38740
301.5–302.5	8585 ± 40	9240.5 ± 139.5	KIA 43853
370.0–373.0	9490 ± 50	10350.5 ± 133.5	KIA 38701

[a] Müller et al. (2012).

level. Fragmentation (%) was calculated following the procedure by Pfuhl and Shackleton (2004) (Eq. (1)):

$$\text{Fragmentation}(\%) = \frac{\#\text{planktic foraminiferal fragments/g}}{(\#\text{pl.foram.fragments/g})/3 + \#\text{pl.foram.tests/g}} \times 100 \quad (1)$$

Stable isotope analysis was carried out from picked planktic foraminiferal species *N. pachyderma* and *T. quinqueloba* (ca 25 specimens each, size fraction 100–250 μm) as well as the benthic foraminifer species *Cibicidoides wuellerstorfi* (ca 10 to 15 specimens, size fraction 250–500 μm). Tests were crushed and well-mixed prior to measurements using a Finnigan MAT 253 mass spectrometer system and a Kiel IV Carbonate Preparation Device. All measurements were calibrated to Pee Dee Belemnite (NBS 19). Analytical accuracy was <0.06% for δ^{18}O and <0.03% for δ^{13}C.

3.2. Transfer functions

The transfer functions by Husum and Hald (2012) have been used to calculate sea subsurface temperatures (SST100) based on planktic foraminiferal fauna assemblages. This approach is based on a comparison between modern oceanographic data (summer SST at 100 m depth) and compositions of planktic foraminifer fauna in surface sediment samples from the northern North Atlantic and the Fram Strait. The method by Husum and Hald (2012) applies a size fraction of >100 μm. For the transfer function, the procedure of the weighted averaging partial least squares (WA-PLS) has been

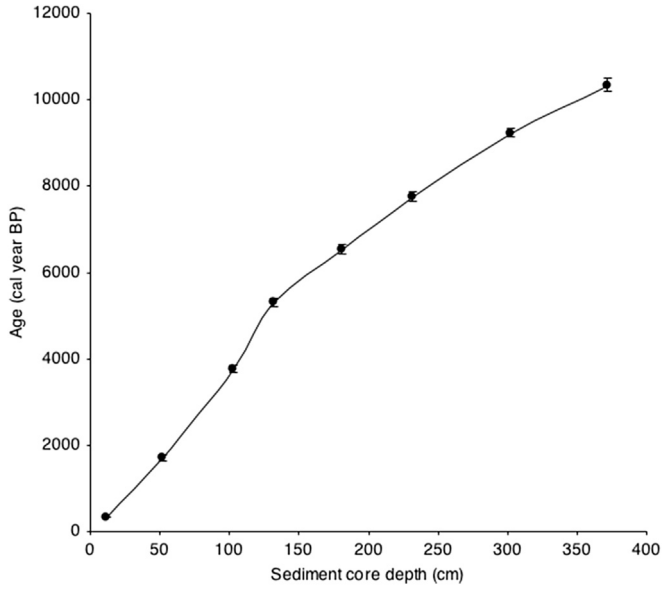

Fig. 3. Age-depth model of core 723-2 including 2σ-uncertainties. Upper six dates have been published previously by Müller et al. (2012) (for details see Table 1).

chosen, with a most precise estimate of root mean squared error of prediction (RMSEP) of ±0.47 °C (WA-PLS component 3). Cross-validation for the latter was provided with leave-one-out ('jack-knifing') (Ter Braak and Juggins, 1993; Birks, 1995). The temperatures applying the technique suggested by Husum and Hald (2012) were calculated using the C2 software (Juggins, 2010).

In addition, SIMMAX summer SST reconstructions for 50 m water depth from core MSM5/5-712-2 (Werner et al., 2013) have been selected. The SIMMAX transfer function was developed to improve SST reconstruction in polar and subpolar regions (Pflaumann et al., 1996, 2003). It represents a sophisticated version of the modern analogue technique (MAT; Prell, 1985). In our case, the foraminiferal core-top reference data set restricted to the North Atlantic sector was linked to the modern 50 m-water depth SST (Locarnini et al., 2010). For our interpretation, only non-distance weighted summer SST for the Nordic Seas (north of 60°N) yielded standard deviation of the residuals equal to 1.6 °C which can be considered as a good accuracy at the cold end of the temperature data set where an accuracy of any method tends to decrease (e.g., Pflaumann et al., 2003; Kandiano et al., 2004).

3.3. Ice-rafted debris

Lithic grains of samples were counted on a representative split (>100 grains) in the size fraction 150–250 mm. Rounded and angular quartz grains were separately specified while counting.

3.4. Organic geochemical analyses

Determination of organic geochemical bulk parameters (total organic carbon, TOC; carbonate content, $CaCO_3$) and biomarker analyses were carried out following Müller et al. (2012). Briefly, for TOC and $CaCO_3$ measurements freeze-dried and homogenised sediments were analysed by means of a carbon–sulphur determinator (CS-125, Leco) and a CNS analyser (Elementar III, Vario), respectively. For lipid biomarker analyses ca 4 g of freeze-dried and homogenised sediment were extracted by an Accelerated Solvent Extractor (DIONEX, ASE 200; 100 °C, 5 min, 1000 psi) using dichloromethane:methanol (2:1 v/v). Separation of hydrocarbon and sterol fractions from the total lipid extract was achieved via open column chromatography using hexane and methylacetate:*n*-hexane (20:80 v/v), respectively. Coupled GC–MS analyses (Agilent 6850 GC, Agilent 5975 C VL mass selective detector) were performed for the identification and quantification of highly branched isoprenoids and sterols. For further analytical details we refer to Müller et al. (2012) and Müller and Stein (2014). While the DIP_{25} index is calculated from IP_{25} and C_{25}-HBI diene GC–MS peak areas, PIP_{25} indices used here were calculated following Müller et al. (2012).

4. Results

4.1. Planktic foraminifer assemblages and fragmentation

N. pachyderma percentages are relatively high from ca 12 to 10.6 cal ka BP and strongly decrease thereafter while *T. quinqueloba* becomes dominant (>80%) at this time (Fig. 4a, b). Minimum abundance of *N. pachyderma* is noted at ca 10 cal ka, thereafter it returns stepwise. Local maxima of *N. pachyderma* between ca 10 and 5 cal ka BP occur at 9.4, 8.5–8.1, 6.9, 6–5.8, and at ca 5 cal ka BP. Accordingly, during other times, *T. quinqueloba* is dominant in the foraminiferal record. The significant increase of *N. pachyderma* between 5.5 and 5 cal ka BP is remarkable as thereafter, except for the uppermost sample, *N. pachyderma* stays at relatively high levels (75–50%). Slight increases of *T. quinqueloba* are noticeable during the later part of the record: at ca 2 and 1.5 cal ka BP (40%) and during the past decades where *T. quinqueloba* reaches >50% and *N. pachyderma* decreases to <30%.

Planktic foraminifer concentration and fluxes are low until 10.6 cal ka BP but higher and highly variable during the early Holocene part of the record until ca 5.2 cal ka BP (Fig. 4c, d). Thereafter, the concentration (ind./g dry sediment) slightly decreases and remains relatively stable except for single peak values at ca 2 cal ka BP and a low value at ca 1.5 cal ka BP. Fluxes slightly decrease after 5.2 cal ka BP and display the same trends as the concentrations.

Planktic foraminifer fragmentation reaches highest values between 4.8 and 3.5 cal ka BP (Fig. 4e). Other shorter maxima are noticed after 10 cal ka BP, around 11 cal ka BP, before 8.5 cal ka BP, and between 7.5 and 6 cal ka BP. Fragmentation is low after 3.5 cal ka BP.

4.2. Sea-subsurface temperature reconstruction

Both ecological transfer functions discussed in this paper are based on comprehensive data sets of modern foraminiferal assemblages in the Fram Strait area and the northern North Atlantic (Pflaumann et al., 1996; 2003; Husum and Hald, 2012). Fig. 4f shows Holocene variability of subsurface water mass temperatures in sediment core 723-2. SST100 are rather low at 12 cal ka BP but gradually increase from 2 to 4 °C until ca 10.7 cal ka BP. A further steep increase in SST100 is noted thereafter when temperatures rise to maximum values of 5 and 6 °C around ca 10.2 cal ka BP. While gradually decreasing temperatures stay always above 5 °C until ca 8.6 cal ka BP, from 8.5 to 8.1 cal ka BP a two-phase low in SST100 is observed with minimum values of less than 4.5 °C at 8.5 and 8.1 cal ka BP and a slightly warmer phase of ca 4.9 °C in between. After 8.1 cal ka BP, temperatures return to values between 5 and 5.5 °C until ca 7.5 cal ka BP. Thereafter, a stepwise rather steep decrease in SST100 is found towards minimum temperatures of 3.5 °C at 6.6 cal ka BP. Another warming follows, though with high fluctuations, until ca 6 cal ka BP (up to 5 °C). After 6 cal ka BP, temperatures drop stepwise to 3 °C until ca 3 cal ka BP. Warmer temperatures are indicated thereafter between 2.5 and 1.0 cal ka BP (on average ca 3.6 °C). Within the uppermost

Please cite this article in press as: Werner, K., et al., Holocene sea subsurface and surface water masses in the Fram Strait – Comparisons of temperature and sea-ice reconstructions, Quaternary Science Reviews (2015), http://dx.doi.org/10.1016/j.quascirev.2015.09.007

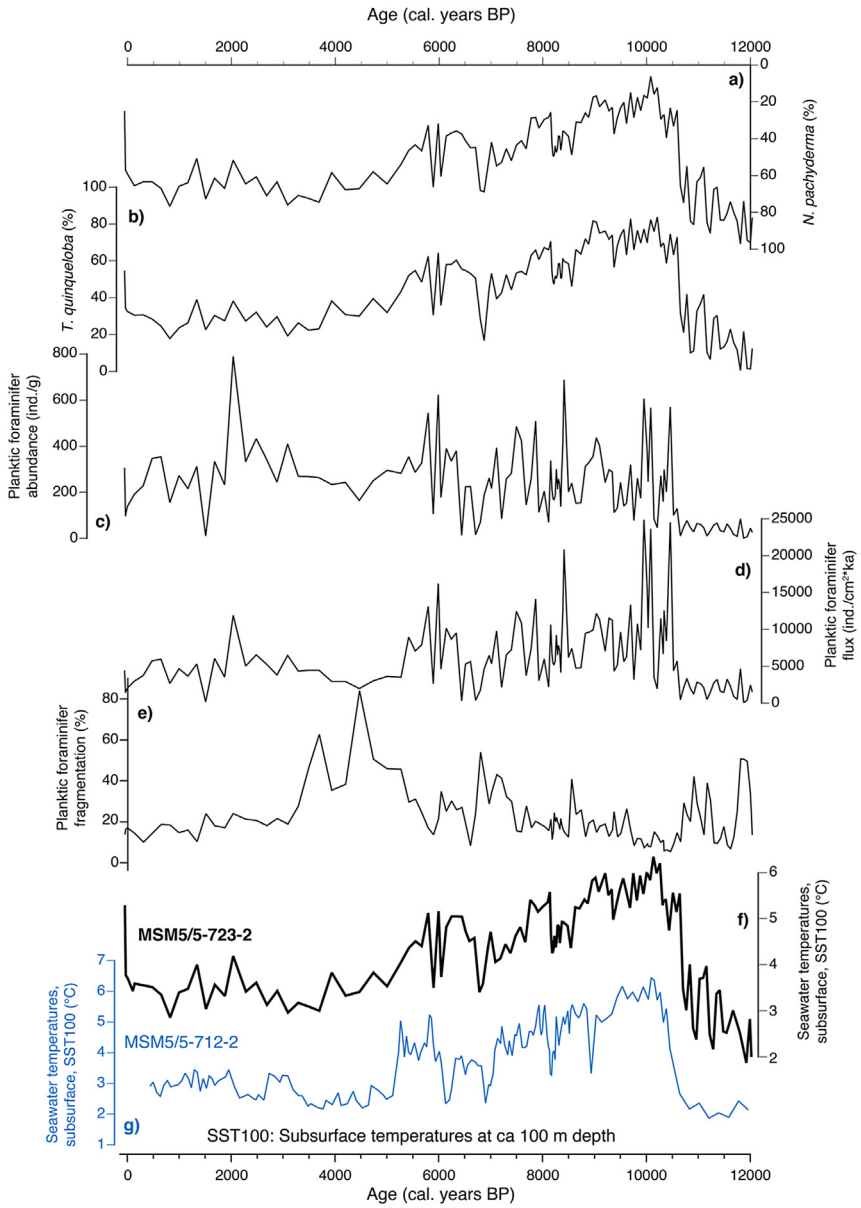

Fig. 4. (a–f) Holocene planktic foraminiferal fauna data from sediment core MSM5/5-723-2 including sea subsurface temperature reconstructions. The relative abundance of *N. pachyderma* (a) is presented on a reverse scale. g) Sea subsurface temperature reconstructions after Husum and Hald (2012) in core MSM5/5-712-2 using foraminiferal planktic data from Werner et al. (2013).

sediments, a strong temperature increase is found (>5 °C) similar to previous findings by Spielhagen et al. (2011) in sediment core MSM5/5-712-1.

Likewise, SST100 were reconstructed from sediment core MSM5/5-712-2 (Fig. 4g) with the same approach indicating similar trends and temperatures, though slight differences are observed between the two sediment cores. Notably are maximum Holocene temperatures of 6.5 °C occurring around 10 cal ka BP which are slightly higher than in 723-2. Early Holocene short-term cooling episodes (between 2.5 and 3.5 °C) are more pronounced in 712-2 than in 723-2 occuring at 9.2, 8.1, 6.9 and 6.1 cal ka BP. After 5.2 cal ka BP a strong decrease in temperatures is noted from 5 to 3 °C. SST100 stay between 2.5 and 3.5 °C during the late Holocene with slightly warmer episodes around ca 3 cal ka BP and from 2 to 1 cal ka BP.

4.3. Foraminiferal stable isotopes

Foraminiferal stable isotope data are shown in Fig. 5. Stable oxygen isotope values of *N. pachyderma* are strongly fluctuating around 12 cal ka BP (2.2–4.6‰) (Fig. 5a). Until ca 11.0 cal ka BP, $\delta^{18}O$ values are relatively high but drastically decrease thereafter. From ca 10.5 to 7.5 cal ka BP *N. pachyderma* $\delta^{18}O$ values are generally lower with respect to the preceding and ensuing intervals, except for a short peak at ca 8.7 and 8.2 cal ka BP. After ca 7.5 cal ka BP, *N. pachyderma* $\delta^{18}O$ values increase until ca 6.5 cal ka BP. A short minimum is noted thereafter while values in general increase again until ca 3.8 cal ka BP. Afterwards a slight but continuous decrease in *N. pachyderma* $\delta^{18}O$ values is noted.

The $\delta^{18}O$ record of *T. quinqueloba* starts at 10.5 cal ka BP (Fig. 5a). Values are highly fluctuating throughout the record. However, in

Please cite this article in press as: Werner, K., et al., Holocene sea subsurface and surface water masses in the Fram Strait – Comparisons of temperature and sea-ice reconstructions, Quaternary Science Reviews (2015), http://dx.doi.org/10.1016/j.quascirev.2015.09.007

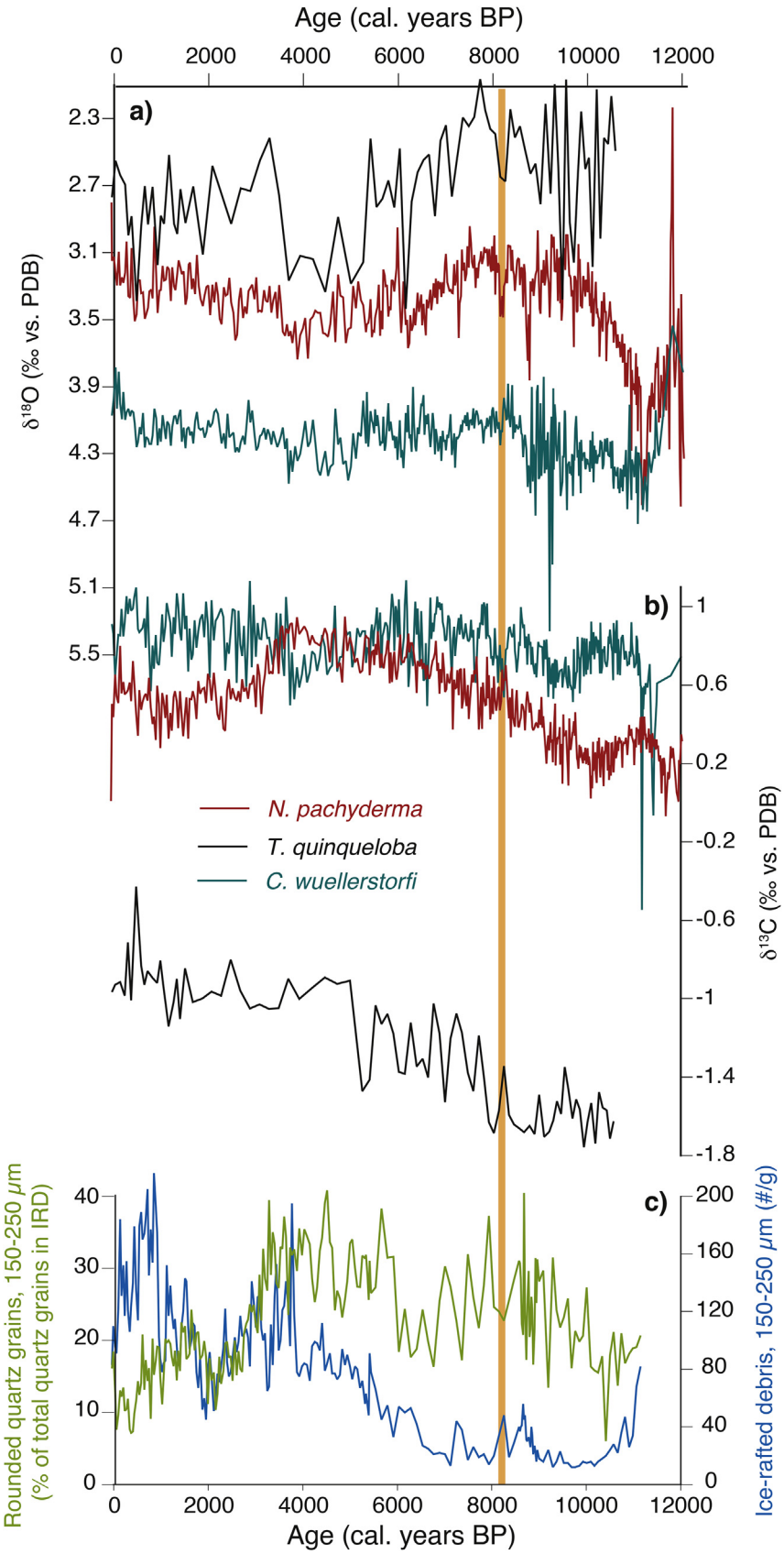

Fig. 5. a, b) Holocene stable isotope data from three foraminifer species in core M5/5-723-2. c) Ice-rafted debris and portion of rounded quartz grains (as calculated from total quartz grains). The orange bar highlights the 8.2 cal ka BP-event (see Section 5.3). (For interpretation of the references to colour in this figure legend, the reader is referred to the web version of this article.).

Please cite this article in press as: Werner, K., et al., Holocene sea subsurface and surface water masses in the Fram Strait – Comparisons of temperature and sea-ice reconstructions, Quaternary Science Reviews (2015), http://dx.doi.org/10.1016/j.quascirev.2015.09.007

general lighter values are noticeable during the early Holocene until ca 5.2 cal ka BP. Strong short-term increases during that period are found before and after ca 10 cal ka BP as well as at ca 6 cal ka BP. A general, less variable increase in *T. quinqueloba* $\delta^{18}O$ values is observed between 5 and 3.5 cal ka BP. Thereafter values decrease with higher variability.

Stable oxygen isotope values of the epibenthic species *C. wuellerstorfi* are highly fluctuating around 12 cal ka BP and are relatively high thereafter until ca 10.5 cal ka BP (Fig. 5a). A stepwise decrease in $\delta^{18}O$ values is noted thereafter with higher fluctuations and an decrease after ca 9 cal ka BP. In the following, $\delta^{18}O$ values are fluctuating around an average of ca 4.1‰ with some increase between 5 and 4 cal ka BP and lighter values since ca 0.5 cal ka BP.

Stable carbon isotopes are shown in Fig. 5b. *N. pachyderma* $\delta^{13}C$ values stay rather low from 12.0 to 10.0 cal ka BP but slightly increase around 11.5 cal ka BP (Fig. 5b). After 10 cal ka BP, a gradual increase is noted lasting until ca 3.8 cal ka BP. A trend to lower values is found thereafter until ca 1 cal ka BP. During the last 1000 years, *N. pachyderma* $\delta^{13}C$ values are slightly increasing again. The youngest $\delta^{13}C$ values are strongly decreasing.

Carbon isotope values of *C. wuellerstorfi* are very low after 12 cal ka BP but strongly increase after 11 cal ka BP (Fig. 5b). Thereafter they stay on a high level with minor fluctuations (local minima found at 10 to 9 and 5.8 to 3.8 cal ka BP) with a trend to slightly higher values in the last 4 cal ka BP. Again, the youngest values are strongly decreasing.

T. quinqueloba $\delta^{13}C$ values are on average 1.5‰ lower and more variable than those of the two other species (Fig. 5b). They generally follow the trends of the *C. wuellerstorfi* record.

4.4. Ice-rafted debris

Lithic particles in the size fraction 150–250 μm reveal a negative trend around 11 cal ka BP (Fig. 5c). However, after ca 9 cal ka BP three significant IRD peaks are noted: after 9, after 8.5, and at ca 7.5 cal ka BP. After 7 cal ka BP, IRD increase stepwise but strongly until ca 4 cal ka BP. A minimum around 2 cal ka BP is followed by higher values in the last millennium.

Percentages of rounded quartz grains are highly variable throughout the record but show a positive trend from 11 to ca 3 cal ka BP (Fig. 5c). A minimum is noted between 7 and 6 cal ka BP. After 3 cal ka BP, values gradually decrease with a minor peak at ca 2 to 1 cal ka BP.

4.5. Biomarker data

TOC and $CaCO_3$ contents as well as concentrations of biomarkers and PIP_{25} and DIP_{25} indices are shown in Fig. 6. A TOC minimum (0.7wt.%) is observed between 12 and 11.7 cal ka BP, which is followed by a significant increase in TOC from 11.5 cal ka BP reaching maximum values (1.8wt.%) at 11 cal ka BP (Fig. 6f). Thereafter variability is low throughout the remainder of the record with values in the range of 1–1.4wt.%. A gradual though slight increase is noted between 7.2 and 0.5 cal ka BP.

$CaCO_3$ content is low (3–5wt.%) until ca 10.5 cal ka BP but increases stepwise thereafter (Fig. 6g). It is highly variable between 8.4 and 8 cal ka BP with local maxima between 7.5 and 7 cal ka BP as well as 6 and 5.5 cal ka BP. Thereafter $CaCO_3$ slightly increases. Noticeable is the high variability with higher values from ca 2.5 cal ka BP.

Concentrations of the phytoplankton-derived biomarkers dinosterol and brassicasterol (Kanazawa et al., 1971; Boon et al., 1979; Volkman, 2006) are highly variable throughout the entire record (Fig. 6d, e). A general increase is observed for dinosterol during the late Holocene. In strong contrast to the phytoplankton biomarkers, IP_{25} concentrations are less variable (Fig. 6c). A distinct decrease in IP_{25} concentrations from maximum values of 0.6 μg/g to 0.1 μg/g OC occurred between 12 and 11.2 cal ka BP. Thereafter, concentrations remain low until ca. 7.2 cal ka BP, when a slight shift to higher values occurred and a successive increase in IP_{25} concentrations is observed for the mid and late Holocene (Fig. 6c).

The DIP_{25} or diene-IP_{25} index which describes the C_{25}-HBI diene to IP_{25} ratio exhibits a relatively high variability (Fig. 6b). Low values of 3 are noted until 11.4 cal ka BP. Between 11 and 6.5 cal ka BP, DIP_{25} values oscillate significantly between minimum values of 3 and maximum values of 15. Less variable and generally decreasing DIP_{25} ratios are observed after 7 cal ka BP (Fig. 6b).

Dinosterol and brassicasterol-based PIP_{25} indices (P_DIP_{25}, P_BIP_{25}; Müller et al., 2011) both show parallel trends of strongly decreasing values from 11.7 to 11 cal ka BP (Fig. 6a). Values stay low (0.3–0.4) with few fluctuations until ca 7 cal ka BP. Noticeable is a short-term minimum at ca 9 cal ka BP and a subsequent maximum between 9 and 8.5 cal ka BP. P_BIP_{25} and P_DIP_{25} indices both increase consistently from 7 to 0.5 cal ka BP, when they reach similarly high values (ca. 0.7–0.8) as observed for 11.7 cal ka BP.

5. Discussion

5.1. (Sub-)surface temperature reconstructions in the eastern Fram Strait area

The sediment record consists of two dominant planktic foraminiferal species that are negatively correlated (Fig. 4a, b): the polar planktic foraminifer species *N. pachyderma* (Simstich et al., 2003) and the subpolar species *T. quinqueloba*, which is indicative for warm and saline Atlantic Water advection (Volkmann, 2000). On average, other planktic foraminifer species only contribute by 4.8% of the entire fauna. The fauna clearly shows polar conditions from 12 to 10.6 cal ka BP when *T. quinqueloba* becomes dominant thereafter (Fig. 4b). Warmer conditions remain until ca 5 cal ka BP when relative abundances of *T. quinqueloba* and *N. pachyderma* become more similar.

We like to note here, that we are aware of the fact that foraminiferal transfer functions are only one of several possible approaches to estimate past seawater temperatures. For our interpretation, we use general trends indicated by temperatures records rather than absolute numbers. Due to the precision limits of these methods, we carefully abstain from over-interpreting small-scale (less than 0.5 °C) changes in temperatures.

The Holocene subsurface water temperature reconstruction of core 723-2 using the 100–250 μm size fraction of planktic foraminifer fauna (Husum and Hald, 2012) strongly aligns with the abundance of the planktic foraminifer species *T. quinqueloba* in the same size fraction (Figs. 4b, f and 7b). These parallel trends can also be observed for sediment core 712-2 (Figs. 4b and 8d), hence it appears that the current reconstructed SST100 are driven mainly by the relative abundance of *T. quinqueloba*. Since presence of *T. quinqueloba* in the eastern Fram Strait area has been related to an increased advection of warmer Atlantic Water (AW) masses (e.g., Carstens et al., 1997; Volkmann, 2000; Pados and Spielhagen, 2014), we conclude the reconstructed temperature variations are caused by the temperature fluctuations due to variable AW contribution rather than fluctuations of the Arctic Front with which *T. quinqueloba* has been associated within the Nordic Seas (Johannessen et al., 1994). It has to be noted that planktic foraminifer fragmentation is high between ca 4.8 and 3.5 cal ka BP (Fig. 4) indicating that less robust species as *T. quinqueloba* may be underrepresented during this interval (cf. Zamelczyk et al., 2012;

Please cite this article in press as: Werner, K., et al., Holocene sea subsurface and surface water masses in the Fram Strait – Comparisons of temperature and sea-ice reconstructions, Quaternary Science Reviews (2015), http://dx.doi.org/10.1016/j.quascirev.2015.09.007

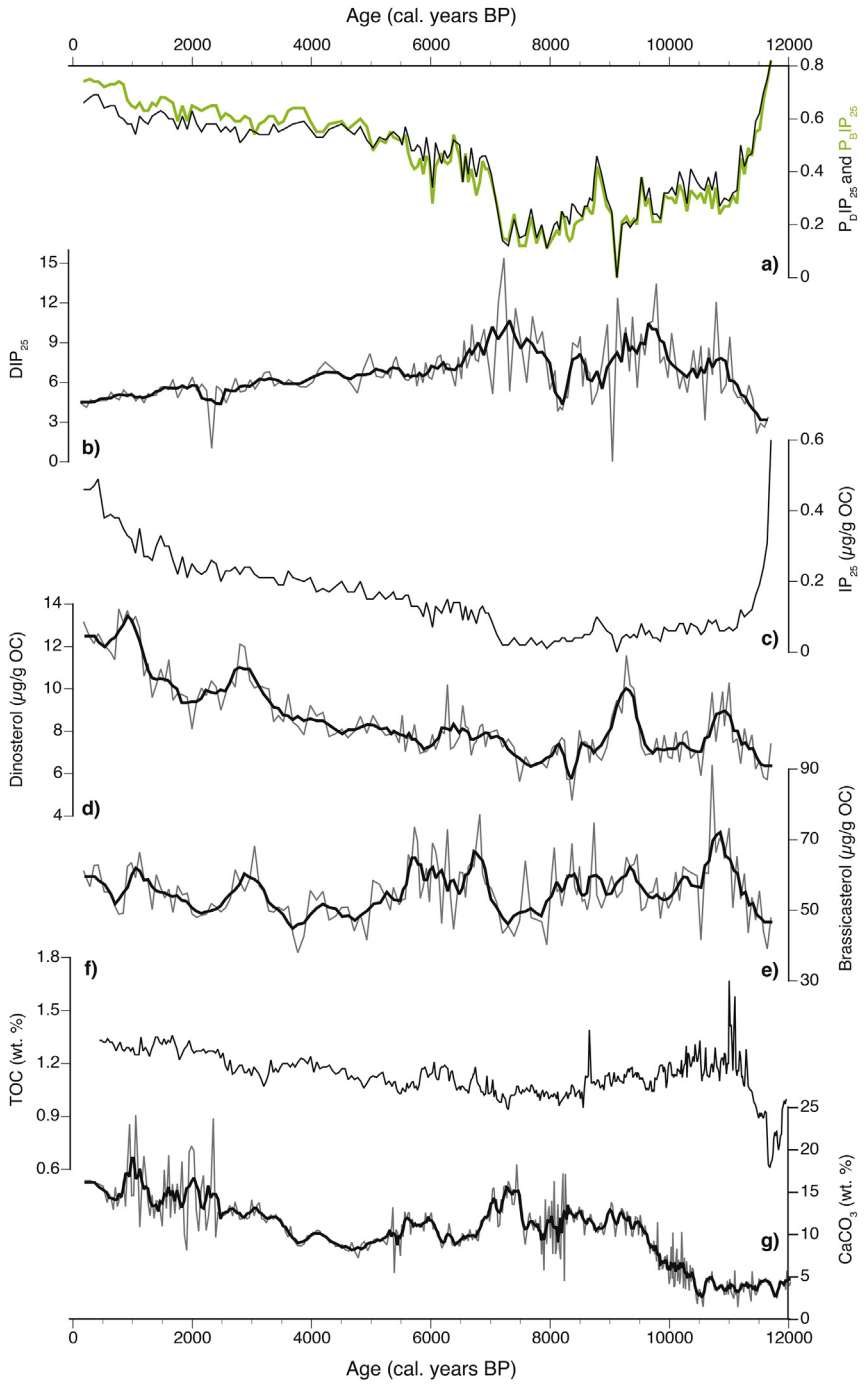

Fig. 6. Holocene organic geochemical bulk and biomarker data of core MSM5/5-723-2. In b, d, e, and g the 5-point moving average is shown in black.

2013) resulting in too low temperatures reconstructed during this time. However, the decrease both in *T. quinqueloba* percentages and carbonate concentration after 5 cal ka BP are parallel to an increase in $\delta^{18}O$ of *T. quinqueloba* (Figs. 4b, 6g and 7e). This supports a conclusion on generally colder surface water conditions not only during the time of the pronounced increase in planktic foraminifera fragmentation at 4.8–3.5 cal ka BP but also during short-term increases of fragmentation at 11.2–10.5, 8.6, and 7.5–6.6 cal ka BP when increased planktic $\delta^{18}O$ indicate contributions of cold waters (Fig. 7d, e and h). A selective removal of dissolution-prone species such as *T. quinqueloba* by CO_2-enriched, low-pH Arctic waters has been discussed by Zamelczyk et al. (2014). Likewise, we are able to use the fragmentation proxy here as an additional indicator of rather cold surface water conditions due to enhanced impact of cold, corrosive Arctic surface waters to the study area. Whether subpolar foraminifera were present in the area or not, AW advection was likely weakened at the core location during these intervals, and dominant Arctic surface waters might have caused partial dissolution of foraminifera.

A similar temperature reconstruction for the past ca 9000 years has been previously achieved by means of the SIMMAX transfer function for sediment core 712-2 (Fig. 8d; Werner et al., 2013) derived from a slightly coarser size fraction of counted planktic foraminifera (150–250 µm). Calculated water temperatures at 50 m

Please cite this article in press as: Werner, K., et al., Holocene sea subsurface and surface water masses in the Fram Strait – Comparisons of temperature and sea-ice reconstructions, Quaternary Science Reviews (2015), http://dx.doi.org/10.1016/j.quascirev.2015.09.007

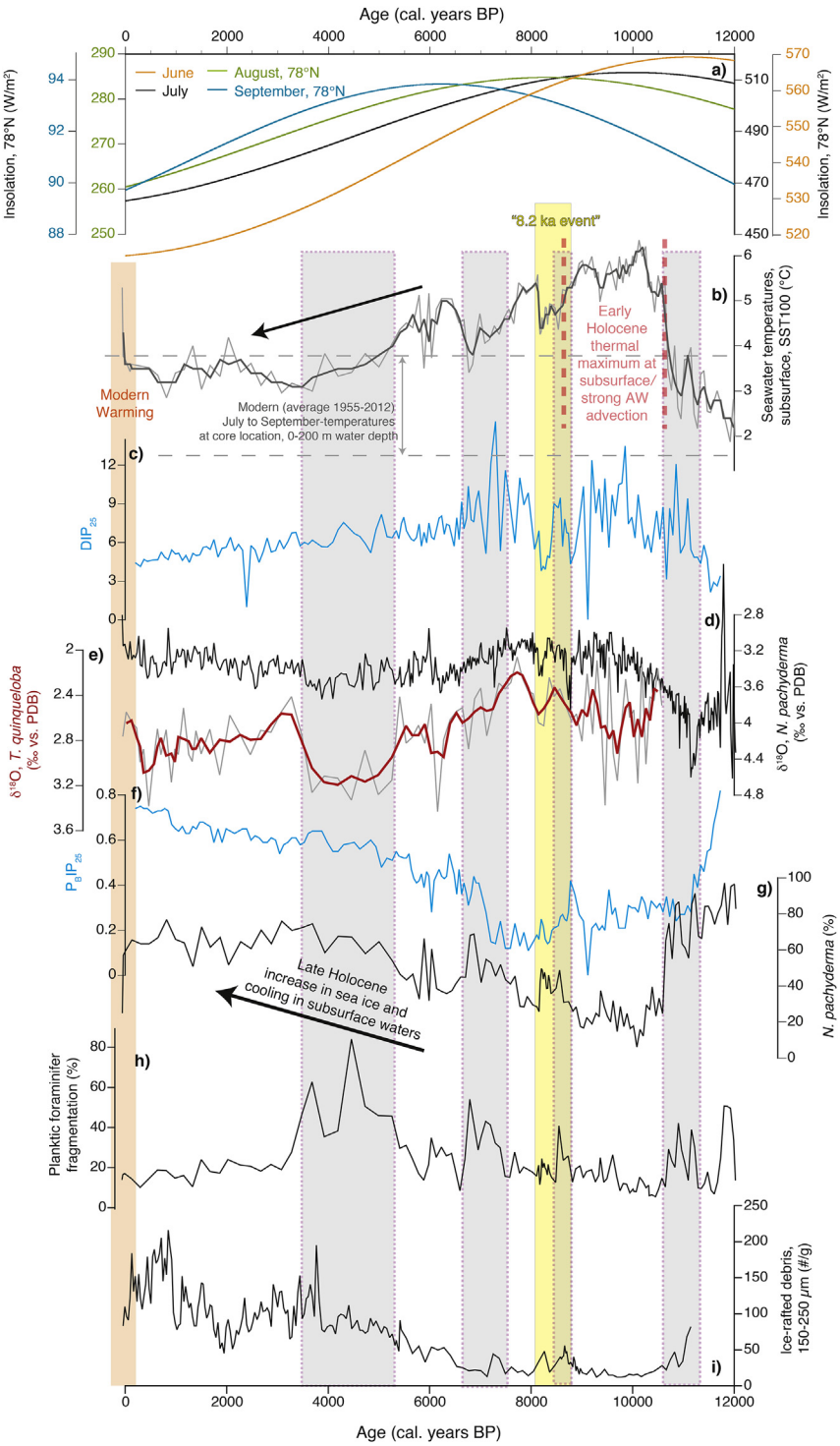

Fig. 7. a) Insolation at 78°N for June, July, August, and September (Laskar et al., 2004). b) Reconstructed SST100 (light grey) including 3-point running means (dark grey; Husum and Hald, 2012). c) DIP_{25} index derived from biomarker data. d) *N. pachyderma* stable oxygen isotopes. e) *T. quinqueloba* stable oxygen isotopes incl. 3-point average mean. f) PBIP25 index derived from biomarker data and g) *N. pachyderma* percentages. h) Fragmentation of planktic foraminifer tests and i) ice-rafted debris. Grey bars refer to periods when elevated fragmentation has been found. The yellow and orange bars highlight data linked to the 8.2 cal ka BP-event (see Section 5.3) and the modern warming, respectively. (For interpretation of the references to colour in this figure legend, the reader is referred to the web version of this article.).

water depths (furthermore referred to as SST50) indicate the same feature being controlled by abundance of the two dominant species *T. quinqueloba* and *N. pachyderma*.

When comparing trends and absolute numbers of the past ca 9000 years of both temperature reconstructions, in general SST50 during the early Holocene do not reveal large differences from reconstructed SST100 (Fig. 8d). There are, however, differences noted during colder events when SST100 indicate slightly higher temperatures than SST50 (about 0.5–1 °C difference at ca 7.8, 7.5, 6.9, 6.1, 5.2, 5–4.5 and 4–3.5 cal ka BP). For one, this difference may

Please cite this article in press as: Werner, K., et al., Holocene sea subsurface and surface water masses in the Fram Strait – Comparisons of temperature and sea-ice reconstructions, Quaternary Science Reviews (2015), http://dx.doi.org/10.1016/j.quascirev.2015.09.007

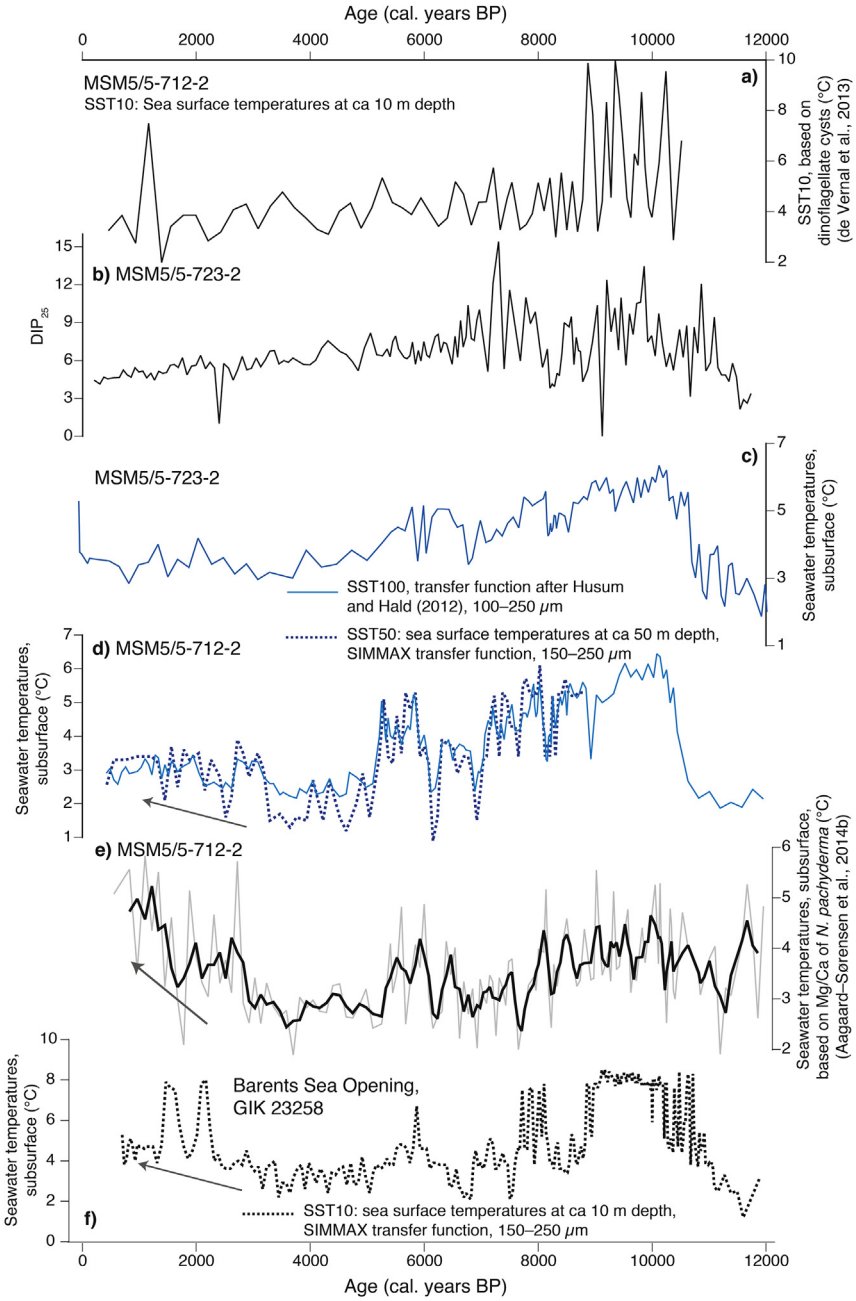

Fig. 8. a) Summer surface water temperatures reconstructed from dinocyst assemblages in core MSM5/5-712-2 (de Vernal et al., 2013; data available on http://www.geotop.ca/en/liste-des-sites/1079-msm712.html). b) DIP25 index derived from biomarker data for core 723-2. c) Reconstructed SST100 in core 723-2. d) Reconstructed SST in core 712-2 (blue solid line SST100; dark blue dashed line SST50 (Werner et al., 2013). e) Reconstructed SST based on Mg/Ca data of *N. pachyderma* (Aagaard–Sørensen et al., 2014b). f) Reconstructed SST10 in core GIK23258 (Sarnthein et al., 2003). (For interpretation of the references to colour in this figure legend, the reader is referred to the web version of this article.).

be attributed to the different temperatures at the different water depths used in the reconstructions, and thus cold fresh Arctic waters may have a higher impact to the shallower SST50 reconstruction. Predominantly, this difference is likely related to the higher presence of small-sized *T. quinqueloba* specimens in the sediment fraction considered by the Husum and Hald (2012) reconstruction while SIMMAX estimates are based on a coarser size fraction. This is good in agreement with findings by Bauch (1994) that average *T. quinqueloba* size is reduced under lower temperatures. Higher abundance of small-sized specimens of *T. quinqueloba* during colder periods has also been noted by previous studies in the area (e.g., Bauch et al., 2001; Kandiano and Bauch, 2002; Nørgaard-Pedersen et al., 2007). We therefore strongly support the recommendation of earlier works (e.g., Kandiano and Bauch, 2002) to include smaller-sized planktic foraminifera in temperature reconstructions for areas with colder water masses.

In addition, occurrence of *T. quinqueloba* within the nutrient-rich marginal ice zone in the Fram Strait has also been discussed previously (e.g., Carstens et al., 1997; Pados and Spielhagen; 2014). Preference of depth habitats of *T. quinqueloba* but also of *N. pachyderma* were associated with depth of maximum food availability, in particular the position of the deep chlorophyll maximum (Kohlfeld et al., 1996; Pados and Spielhagen, 2014). Maximum abundance of *T. quinqueloba* may thus be used in

Please cite this article in press as: Werner, K., et al., Holocene sea subsurface and surface water masses in the Fram Strait – Comparisons of temperature and sea-ice reconstructions, Quaternary Science Reviews (2015), http://dx.doi.org/10.1016/j.quascirev.2015.09.007

addition to conclude on nutrient-rich subsurface waters especially during the early Holocene when *T. quinqueloba* reached abundances of >80% in eastern Fram Strait (Fig. 4b).

5.2. Early Holocene thermal maximum conditions in surface to subsurface water conditions

A retreat of spring sea ice and icebergs due to rising sea surface temperatures in the earliest phase of the Holocene is supported by decreasing IRD content and a significant drop in P_BIP_{25} and P_DIP_{25} values with coincidently rising DIP_{25} values, the latter indicative for surface water temperatures SST10 (Figs. 6 and 7). Elevated and even maximum concentrations of the phytoplankton-derived biomarkers brassicasterol and dinosterol and low concentrations of the sea ice biomarker IP_{25} between 11 to 10.5 and 9.5 to 9 cal ka BP (Fig. 6c–e) suggest a higher primary productivity in response to a reduced sea-ice cover. However, between 11 and 10.6 cal ka BP, subpolar planktic foraminifer abundance (and thus planktic foraminiferal SST100, 2–4 °C) are still relatively low and strongly fluctuating, a pattern that can be similarly observed in the neighbouring core MSM5/5-712-2 (Aagaard-Sørensen et al., 2014a). The delayed record of subpolar planktic foraminifera may be related to the higher planktic foraminifer fragmentation during that time (Fig. 7h) and a preferential removal of the dissolution-prone *T. quinqueloba* when corrosive low-pH Arctic waters prevailed at the surface in proximity to the summer sea-ice margin. This conclusion may be further supported by low calcium carbonate concentration and low planktic foraminifer flux and abundances (Figs. 4c, d and 6g). A further reason for the disparities between the onset of warming at surface and subsurface waters may also be the difference in maximum Holocene insolation depending on the summer month. Maximum phytoplankton blooms have been observed to occur in spring (May–June) in the northern North Atlantic (Wassmann et al., 1991; Bauerfeind et al., 1994). Surface water proxies might have responded to the very high radiation maximum in June at ca 11 cal ka BP. As a consequence, by the end of the spring, surface waters might have been nutrient-depleted due to an intense spring phytoplankton bloom, which hence limited later occurring zooplankton blooms, in agreement with Jonkers et al. (2010) suggesting food availability as one of the major controls on planktic foraminifer fluxes. Maximum occurrence of planktic foraminifers may therefore be linked only to the time around 10 cal ka BP when maximum insolation occurred later during summer (Fig. 7) and more nutrients might have been still available in (sub-)surface waters. .

Accordingly, SST100 only rapidly increased to maximum values at 10.6 ka, which was significantly later than the decrease in the IP_{25} indices, and clearly after the early peaks in Dinosterol, Brassicasterol, and DIP_{25}. At the same time, $\delta^{13}C$ of *N. pachyderma* is rather low in both cores from the Fram Strait (this study; Aagaard-Sørensen et al., 2014a). Low $\delta^{13}C$ values may be related to weak ventilation of the water masses inhabited by *N. pachyderma* (Spielhagen and Erlenkeuser, 1994). Werner et al. (2013) suggested a deeper habitat depth of *N. pachyderma* in less ventilated water masses potentially due to the strong prevalence of fresh and cold sea-ice derived water masses at the surface, which might have been the case during the earliest part of the Holocene.

The drastic increase in *T. quinqueloba* and SST100 at 10.6 cal ka BP may primarily be explained by a shift in water mass contribution around 10.6 cal ka BP which only occurred within about 60 years, similar to the amplitude and rate of change in subsurface water temperatures in the eastern Fram Strait during the last ca 120 years (Spielhagen et al., 2011; see also Fig. 7b). From both decreased IRD contents and planktic foraminifer fragmentation since ca 10.6 cal ka BP we conclude on a retreat of the sea ice margin to a position north of the core location and a subsequent strong warming/prevalence of warm Atlantic Water at surface to subsurface depth from 10.6 cal ka BP onwards. To a large extent, this may be caused by a maximum of northward heat advection at ca. 10 cal ka BP as concluded by Risebrobakken et al. (2011) from seawater temperature reconstructions in the Nordic Seas and Barents Sea.

By far, the large amplitude of 3–10 °C in summer SST reconstructed by dinocysts (de Vernal et al., 2013) cannot be reproduced by foraminifer-derived reconstructions of maximum subsurface temperatures 5–6 °C between 10.6 and 9.0 cal ka BP. This difference in amplitude could be explained by e.g., a highly variable stratification with subsurface waters of more or less constant temperatures but highly variable surface water temperatures but also by differences between proxies in seasonality or their depth habitats. Low values and little variability seen in the sea-ice indicators shown here, however, suggest rather stable conditions with a the study sites. Stable conditions during the critical interval are as well reported by reconstructions from the Nordic Seas (Risebrobakken et al., 2011).

A gradual decrease in foraminiferal water temperatures can be noted soon after ca 10 cal ka BP. This might be partially related to decreasing July insolation and coherent cooling of surface waters as well as consequences of an expanded marginal ice zone (Fig. 7a, i). However, strong Atlantic Water advection likely prevailed dominant at subsurface depth which was also indicated further on the Western Svalbard slope (Rasmussen et al., 2013).

Between ca 10 to 9 cal ka BP, surface and subsurface water proxies, all indicate higher seawater temperatures (Fig. 8a–c). Regardless of the very high temperatures, the SST10 reconstruction based on dinoflagellate cysts in core 712-2 indicates higher, though strongly fluctuating summer month surface water temperatures at 10 to 9 cal ka BP (de Vernal et al., 2013, Fig. 8a). Thus, from similar temperature trends indicated by surface (biomarkers, dinocysts-based) and subsurface (foraminiferal-derived) proxies, we conclude on the presence of a thick and warm summer mixed layer at least until ca 9 cal ka BP with probably limited stratification within the uppermost water column. This thick layer of northward advected strong Atlantic Water likely occupied the uppermost ca 200 m including near-surface waters in the eastern Fram Strait area. Maximum insolation during early summer (June and July, Fig. 7a) probably played an important additional role.

From studies on the shelf and slope of the Western Svalbard margin, Rasmussen et al. (2013) attribute differences in surface to subsurface water temperatures to the variable influence of polar and melt waters derived from inland and east of Spitsbergen. They find strong stratification of the upper water column until ca 9.6 cal ka BP with Arctic and melt waters at surface (30–100 m depth) and warm Atlantic Water below. Apparently, water masses in the eastern Fram Strait further off the Western Svalbard shelf were not as much influenced from these cold water masses found at the surface on the shelf and slopes.

Dinocyst-derived summer surface temperatures suggest an abrupt shift from highly variable and generally warmer to less variable and overall cooler SST10 after ca 9 cal ka (Fig. 8a; de Vernal et al., 2013). Such a rapid sea surface cooling is, however, not reflected in the biomarker records. Slightly decreasing IP_{25} and PIP_{25} values even seem to refer to an ongoing retreat of the sea ice until 7 ka BP, when a distinct rise in PIP_{25} values and generally decreasing DIP_{25} ratios indicate a successive re-expansion of sea ice and decreasing SST10, respectively (Fig. 7c, f). The disparities between the different surface water proxies (biomarkers versus dinocysts) remain unclear at this point. To a certain extent they might not be equally sensitive to environmental changes. Dinocyst data reflect surface water changes in the summer season while IP25 reacts to ice coverage. Furthermore, the strong fluctuations in the dinocyst-

Please cite this article in press as: Werner, K., et al., Holocene sea subsurface and surface water masses in the Fram Strait – Comparisons of temperature and sea-ice reconstructions, Quaternary Science Reviews (2015), http://dx.doi.org/10.1016/j.quascirev.2015.09.007

derived SST10 record may also be caused by changes in nutrient availability (Devillers and de Vernal, 2000).

From latitudinal and temporal discrepancies of alkenone versus foraminiferal-derived seawater temperature reconstruction in the Nordic Seas and Barents Sea, Risebrobakken et al. (2011) discussed the separate roles of maximum insolation and strong oceanic heat advection during the early Holocene with different impacts to surface and subsurface water layers. While maximum northward heat advection (as concluded from subsurface-inhabiting planktic foraminiferal temperatures) occurred already at 10 cal ka BP, the summer mixed layer (indicated by alkenone-derived temperatures) in the Nordic Seas seems to be influenced by maximum insolation slightly later from ca. 9 to 6 cal ka BP (Risebrobakken et al., 2011). For their argumentation, the authors used August insolation with a Holocene maximum around ca 8 cal ka BP. Maximum June and July insolation, however, occurred earlier around 11 to 10 cal ka BP, respectively. In addition, June maximum radiation was higher compared to insolation maxima of later summer months (Fig. 7). To date there are only few studies available on the seasonal cycle of planktic foraminifera from the northern part of the North Atlantic (e.g., Stangeew, 2001; Jonkers et al., 2010; 2013). From the Irminger Sea, Jonkers et al. (2010) report on a bimodal flux pattern of *N. pachyderma* (May–June and late summer) but one broad pulse of *T. quinqueloba* fluxes during summer with a maximum in late September. This pattern may be different both for the Fram Strait and during the early Holocene. Thus, one reason why we do not see a clear separation of surface and subsurface maximum water temperatures during the early part of the early Holocene may be the difference in the seasonal cycle of planktic foraminifera maximum fluxes at different latitudes.

5.3. Pronounced shifts in surface to deepwater proxy records during the '8.2 ka' climate anomaly

A sudden negative trend, concurrent to the freshwater outburst of the glacial lake Agassiz (e.g., Barber et al., 1999), is obvious for few hundred years in foraminiferal temperatures at ca 8.5 and 8.2 cal ka BP with subsurface water temperatures below 4.5 °C (Fig. 7b). This trend is accompanied by local maxima in $\delta^{18}O$ values of *N. pachyderma* and *T. quinqueloba* as well as in ice-rafted debris (Fig. 7d, e and h). Furthermore, a decrease in the dinosterol concentration and in DIP_{25} at ca 8.2 cal ka BP are noted, the latter suggesting decreased surface water temperatures (Fig. 6b, d). We also find slightly reduced amounts of rounded (versus angular) quartz grains during the time of the anomaly (Fig. 5c). This might indicate increased sediment supply of glacial/subglacial origin rather than of ocean-reworked material from beaches etc. to have contributed to ice-rafted debris during that time. We like to note that some of the proxies mentioned above indicate short-term shifts of the same or larger amplitude already between 8.8 and 8.7 cal ka BP (Fig. 5) which may be of rather local origin. As for the cooling around 8.2 cal ka BP, similar features have been found in the neighbouring core 712-2 (Werner et al., 2013) with cool surface and subsurface water conditions around 8.2 cal ka BP we suggest a rather strong impact of the North Atlantic meltwater event to the eastern Fram Strait area.

As discussed in earlier studies (e.g., Kleiven et al., 2008), a coeval shift of water mass conditions is also obvious by indicators of bottom waters. Local minima of carbon isotope values of *C. wuellerstorfi* in sediment core MSM5/5-723-2 (Fig. 5b) but even more pronounced in sediment core MSM5/5-712-2 (Werner et al., 2013) at ca 8.3 and 8.2 cal ka BP, suggest a change in the chemistry also of the deepwater at the site which may be linked to reduced North Atlantic Deep Water renewal further south (Kleiven et al., 2008). Interestingly, the low values in benthic foraminiferal carbon isotopes are accompanied by local increases of $\delta^{13}C$ of *N. pachyderma* and *T. quinqueloba*. Since the signal appears in all foraminiferal $\delta^{13}C$ records of cores MSM5/5-723-2 and MSM5/5-712-2 we assume a change in seawater origin had affected the entire water column in eastern Fram Strait during the 8.2 cal ka BP event.

5.4. Decoupling of surface from subsurface water conditions during the late Holocene

Decreasing insolation during the late Holocene led to changes in water mass properties in the eastern Fram Strait such as a surface cooling accompanied by extended sea-ice extent (Müller et al., 2012; Werner et al., 2013). Extended sea-ice extent in the Fram Strait during the so-called Neoglacial period might have been the result of, amongst other factors, a high production and subsequent export of Arctic sea-ice with the Transpolar Drift via Fram Strait into the Nordic Seas (Werner et al., 2013). Similar to results from sediment core MSM5/5-712-2 (Werner et al., 2013), a significant decrease in *T. quinqueloba* percentages is noted at ca 5 cal ka BP, which is resembled in estimated SST100 (Fig. 7b). Temperatures reach minimum values of ca 3.1 °C between 4 and 3 cal ka BP, similar to findings of lowest temperatures in the area from 5 to 2 cal ka BP by Rasmussen et al. (2013). In addition, increased fragmentation of planktic foraminifer carbonate shells between ca 4.8 and 3.5 cal ka BP parallel to an increase in $\delta^{18}O$ of *T. quinqueloba* (Fig. 7f and h) point to generally colder subsurface water conditions and weakened AW advection. Higher amounts of rounded quartz grains between 6 and 3 cal ka BP may indicate enhanced entrainment of sediments by sea-ice from the shallow Arctic shelves where river load sediments have been identified as one of the sources for sea-ice sediments (Nürnberg et al., 1994).

While the sea-ice increase during the late Holocene has been extensively discussed in earlier studies (e.g., Müller et al., 2012; Werner et al., 2011, 2013), we like to further focus on the concurrently noted development of subsurface (Atlantic) waters.

From ca 2.5 to 1.0 cal ka BP, slight increases in *T. quinqueloba* percentages and estimated SST100 are noted in both cores from the eastern Fram Strait (this study; Werner et al., 2013). Increasing subsurface water temperatures derived from Mg/Ca ratios of *N. pachyderma* since 3 cal ka BP with a maximum of 5 °C at ca 1.1 ka (Aagaard-Sørensen et al., 2014b, Fig. 8e) furthermore suggest slightly strengthened AW advection in the study area. Evidence for increased AW inflow after 3 ka has been found on the slope and shelf of the Western Svalbard margin (e.g., Rasmussen et al., 2013), in the Franz Victoria Trough (Lubinski et al., 2001), the western Barents Sea (Berben et al., 2014), and in the Nordic Seas (Hald and Aspeli, 1997; Hald et al., 2007; Risebrobakken et al., 2003; 2011; Thornalley et al., 2009). Using data from the western Barents Sea shelf, Sarnthein et al. (2003) attributed an increase of *T. quinqueloba* percentages after 3 ka to a slight strengthening of the meridional overturning circulation during the late Holocene.

The warming in subsurface waters suggested by SST100 reconstructions apparently contrasts the simultaneously occurring denser sea-ice cover on the Yermak Plateau and over core sites 723-2 and 712-2, as reconstructed from sea-ice indicative biomarkers and increased IRD contents (Müller et al., 2009; 2012; this study). Also, SST10 based on dinocysts as well as DIP_{25} values indicate rather cool conditions at the surface likely caused by spreading sea-ice coverage and sea-ice derived freshwater contributions.

The apparent contradiction in surface versus subsurface waters can only be explained by simultaneously existing cold conditions at surface waters and increasing temperatures of the Atlantic Water layer, likely separated by a strong pycnocline during the late

Please cite this article in press as: Werner, K., et al., Holocene sea subsurface and surface water masses in the Fram Strait – Comparisons of temperature and sea-ice reconstructions, Quaternary Science Reviews (2015), http://dx.doi.org/10.1016/j.quascirev.2015.09.007

Holocene. The strong stratification of the upper water masses was likely caused by longer winters due to the reduced solar forcing (Fig. 7a) and thus increased seasonality (Berben et al., 2014).

As one possible explanation, the noted increases of late Holocene Atlantic Water advection at various sites in the northern North Atlantic may be related to the variable strength of the North Atlantic Current that was previously explained by dynamic changes in the relative contributions of water masses of the North Atlantic subpolar gyre (SPG) and subtropical gyre (STG) during the past and present (Hátún et al., 2005; Thornalley et al., 2009; Born et al., 2011; Montero-Serrano et al., 2013). Freshwater inputs to the Labrador Sea can prevent deep convection and reduce the SPG circulation resulting in enhanced northward flow of North Atlantic Drift waters which have entrained warmer and saline STG waters (Hátún et al., 2005). Thornalley et al. (2009) found evidence for such linkage throughout the major part of the Holocene in the northeast North Atlantic. The authors identify a negative relationship between Holocene salinity variations south of Iceland and in the Labrador Sea where phases of strong inflow of warm and saline Atlantic Water coincided with a SPG weakened by freshening.

Likewise, the described process holds an explanation for the apparent stratification in the eastern Fram Strait with warmer Atlantic Water temperatures versus surface-water cooling during the late Holocene. Increased sea-ice presence likely caused an effective freshening of surface waters not only in the Fram Strait but also in the Nordic Seas and in the region of the subpolar gyre. We suppose that this freshening caused a late Holocene weakening of the SPG, thereby allowing for enhanced northward transport of heat and salt by the North Atlantic Current eventually affecting strong Atlantic Water advection through the eastern Fram Strait region from 2.5 to 1.0 cal ka BP.

6. Summary

Holocene subsurface water temperature reconstructions of two sediment cores in the eastern Fram Strait following the approach by Husum and Hald (2012) based on planktic foraminifer fauna in size fraction 100–250 μm strongly align with the abundance of the planktic foraminifer species *T. quinqueloba* in the same size fraction.

During warmer periods, sea subsurface temperatures estimated by the Husum and Hald (2012) approach are similar to previously SST50 reconstructions estimated by the SIMMAX transfer function (Pflaumann et al., 1996; 2003). However, during colder periods and events, the Husum and Hald (2012) method indicates higher SST100 due to a higher presence of small-sized *T. quinqueloba* specimens in sediment samples. We therefore strongly agree with earlier recommendations to preferably include smaller-sized planktic foraminifera into temperature reconstructions in the Fram Strait area.

For the first time, DIP_{25} values have been directly compared to reconstructed ocean temperature trends. Similar temperature trends as revealed by surface (biomarkers, dinocysts-based) and subsurface (foraminiferal-derived) proxies indicate the presence of a deep and warm summer mixed layer influenced by northward advected strong Atlantic Water between ca 10 and 9 cal ka BP with limited stratification within the uppermost water column. This warm and supposedly nutrient-rich Atlantic layer likely occupied the uppermost ca 200 m including near-surface waters in the eastern Fram Strait area and was additionally influenced by maximum early summer (June–July) insolation as the sea-ice extent for the period between ca 11 to 8.5 cal ka BP was strongly limited.

During the late Holocene, upper water mass stratification significantly strengthened in the eastern Fram Strait with warmer Atlantic Water advection at the subsurface, cold and fresh polar waters at surface water depth, and a pronounced pycnocline prevailing in between. Increased sea-ice presence likely caused an effective freshening of surface waters not only in the Fram Strait but also in the Nordic Seas and in the region of the subpolar gyre. Increasing supply of sea-ice derived polar freshwaters might have led to a weakening of the subpolar gyre activity and allowed for enhanced northward transport of heat and salt by the North Atlantic Current. Eventually, the strengthened North Atlantic Current probably intensified northward Atlantic Water advection through the eastern Fram Strait region into the Arctic Ocean from 2.5 to 1.0 cal ka BP.

Acknowledgements

We thank the science party and crew onboard RV “Maria S. Merian” during the expedition MSM5/5 for retrieving the sediment core. For laboratory assistance, we thank Marieke Göser, Antonia Hofmann, Jan Oesterwalbesloh, David Poggemann, and Torben Struve. We kindly acknowledge Lulzim Haxhiaj for technical assistance on stable isotope measurements. H. Christian Hass provided one of the additional AMS ^{14}C datings. The German Research Foundation (DFG) provided financial support of KW, JM, and RFS within the Priority Programme 1266 (INTERDYNAMIC, Project HOVAG). KW was furthermore funded through the Byrd Foundation and NSF P2C2 Grant (Award No. 1404370). The manuscript benefited from productive discussion with Steffen Aagaard-Sørensen. Constructive comments by two anonymous reviewers are gratefully appreciated.

Appendix A. Supplementary data

Supplementary data to this article can be found online at http://dx.doi.org/10.1594/PANGAEA.849325.

References

Aagaard Sørensen, S., Husum, K., Werner, K., Spielhagen, R.F., Hald, M., Marchitto, T.M., 2014a. A late glacial-early Holocene multiproxy record from the eastern Fram Strait, Polar North Atlantic. Mar. Geol. 355, 15–26.

Aagaard Sørensen, S., Husum, K., Hald, M., Marchitto, T.M., Godtliebsen, F., 2014b. Sub sea surface temperatures in the Polar North Atlantic during the Holocene: planktic Foraminiferal Mg/Ca temperature reconstructions. Holocene 24, 93–103.

Barber, D.C., et al., 1999. Forcing of the cold event of 8,200 years ago by catastrophic drainage of Laurentide lakes. Nature 400, 344–348.

Bauch, H., 1994. Significance of variability in *Turborotalia quinqueloba* (Natland) test size and abundance for paleoceanographic interpretations in the Norwegian-Greenland Sea. Mar. Geol. 121, 129–141.

Bauch, H.A., Erlenkeuser, H., Spielhagen, R.F., Struck, U., Matthiessen, J., Thiede, J., Heinemeier, J., 2001. A multiproxy reconstruction of the evolution of deep and surface waters in the subarctic Nordic seas over the last 30,000 yr. Quat. Sci. Rev. 20 (4), 659–678.

Bauerfeind, E., von Bodungen, B., Arndt, K., Koeve, W., 1994. Particle flux, and composition of sedimenting matter in the Greenland sea. J. Mar. Syst. 5, 411–423.

Bé, A.W.H., 1977. An ecological, zoogeographic and taxonomic review of recent planktonic foraminifera. In: Ramsay, A.T.S. (Ed.), Oceanic Micropalaeontology. Academic Press, London, UK, pp. 1–100.

Bé, A.W.H., Tolderlund, D.S., 1971. Distribution and ecology of living planktic foraminifera in surface waters of the Atlantic and Indian Ocean. In: Funnel, B.M., Riedel, W.R. (Eds.), The Micropalaeontology of Oceans. Proceedings of the Symposium Micropalaeontology of Marine Bottom Sediments 10-17 September 1967, Cambridge, UK, pp. 105–149.

Belt, S.T., Massé, G., Rowland, S.J., Poulin, M., Michel, C., LeBlanc, B., 2007. A novel chemical fossil of palaeo sea ice: IP_{25}. Org. Geochem. 38 (1), 16–27.

Bengtsson, L., Hodges, K.I., Roeckner, E., 2006. Storm tracks and climate change. J. Clim. 19, 3518–3543.

Berben, S., Husum, K., Cabedo-Sanz, P., Belt, S.T., 2014. Holocene sub-centennial evolution of Atlantic water inflow and sea ice distribution in the western Barents Sea. Clim. Past 10, 181–198.

Birks, H.J.B., 1995. Quantitative palaeoenvironmental reconstructions. In: Maddy, D., Brew, J.S. (Eds.), Statistical Modelling of Quaternary Science Data. Quaternary Research Association, Cambridge, UK, pp. 116–254.

Boon, J.J., Rijpstra, W.I.C., Lange, F.d., de Leeuw, J.W., Yoshioka, M., Shimizu, Y., 1979.

Black Sea sterol - a molecular fossil for dinoflagellate blooms. Nature 277, 125–127.
Born, A., Nisancioglu, K.H., Risebrobakken, B., 2011. Late Eemian warming in the Nordic seas as seen in proxy data and climate models. Paleoceanography 26, PA2207.
Brown, T.A., Belt, S.T., Tatarek, A., Mundy, C.J., 2014. Source identification of the Arctic sea ice proxy IP_{25}. Nat. Commun. 5, 4197.
Cabedo-Sanz, P., Belt, S.T., Knies, J., Husum, K., 2013. Identification of contrasting seasonal sea ice conditions during the younger Dryas. Quat. Sci. Rev. 79, 74–86.
Carstens, J., Hebbeln, D., Wefer, G., 1997. Distribution of planktic foraminifera at the ice margin in the Arctic (Fram Strait). Mar. Micropaleontol. 29, 257–269.
Devillers, R., de Vernal, A., 2000. Distribution of dinoflagellate cysts in surface sediments of the northern North Atlantic in relation to nutrient content and productivity in surface waters. Mar. Geol. 166, 103–124.
De Vernal, A., Hillaire-Marcel, C., Rochon, A., Fréchette, B., Henry, M., Solignac, S., Bonnet, S., 2013. Dinocyst-based reconstructions of sea ice cover concentration during the Holocene in the Arctic Ocean, the northern North Atlantic Ocean and its adjacent seas. Quat. Sci. Rev. 79, 111–121.
Fahl, K., Stein, R., 2012. Modern seasonal variability and deglacial/Holocene change of central Arctic Ocean sea-ice cover: new insights from biomarker proxy records. Earth Planet. Sci. Lett. 351–352, 123–133.
Häkkinen, S., Rhines, P.B., 2004. Decline of subpolar North Atlantic circulation during the 1990s. Science 304, 555–559.
Hald, M., Aspeli, R., 1997. Rapid climate shifts of the northern Norwegian sea during the deglaciation and the Holocene. Boreas 26, 16–28.
Hald, M., Ebbesen, H., Forwick, M., Godtliebsen, F., Khomenko, L., Korsun, S., Ringstad Olsen, L., Vorren, T.O., 2004. Holocene paleoceanography and glacial history of the West Spitsbergen area, Euro-Arctic margin. Quat. Sci. Rev. 23, 2075–2088.
Hald, M., Andersson, C., Ebbesen, H., Jansen, E., Klitgaard Kristensen, D., Risebrobakken, B., Salomonsen, G.R., Sarnthein, M., Sejrup, H.P., Telford, R.J., 2007. Variations in temperature and extent of Atlantic water in the northern North Atlantic during the Holocene. Quat. Sci. Rev. 26, 3423–3440.
Hátún, H., Sandø, A.B., Drange, H., Hansen, B., Valdimarsson, H., 2005. Influence of the Atlantic subpolar gyre on the thermohaline circulation. Science 309, 1841–1844.
Husum, K., Hald, M., 2012. Arctic planktic foraminiferal assemblages: implications for subsurface temperature reconstructions. Mar. Micropaleontol. 96–97, 38–47.
Johannessen, T., Jansen, E., Flatøy, A., Ravelo, A.C., 1994. The relationship between surface water masses, oceanographic fronts and paleoclimatic proxies in surface sediments of the Greenland, Iceland, Norwegian seas. In: Zahn, R., et al. (Eds.), Carbon Cycling in the Glacial Ocean: Constraints of the Ocean's Role in Global Change. Springer, Berlin, pp. 61–85.
Jonkers, L., Brummer, G.-J.A., Peeters, F.J.C., van Aken, H.M., De Jong, F., 2010. Seasonal stratification, shell flux, and oxygen isotope dynamics of left-coiling *N. pachyderma* and *T. quinqueloba* in the western subpolar North Atlantic. Paleoceanography 25, PA2204.
Jonkers, L., van Heuven, S., Zahn, R., Peeters, F.J.C., 2013. Seasonal patterns of shell flux, $\delta^{18}O$ and $\delta^{13}C$ of small and large *N. pachyderma* (s) and *G. bulloides* in the subpolar North Atlantic. Paleoceanography 28, 164–174.
Juggins, S., 2010. Software for Ecological and Palaeoecological Data Analysis and Visualization. C2, Version 1.6.6. University of Newcastle upon Tyne, UK.
Kandiano, E.S., Bauch, H., 2002. Implications of planktic foraminiferal size fractions for the glacial-interglacial paleoceanography of the polar North Atlantic. J. Foraminifer. Res. 32, 245–251.
Kandiano, E.S., Bauch, H.A., Müller, A., 2004. Sea surface temperature variability in the North Atlantic during the last two glacial-interglacial cycles: comparison of faunal, oxygen isotopic, and Mg/Ca-derived records. Palaeogeogr. Palaeoclimatol. Palaeoecol. 204, 145–164.
Kanazawa, A., Yoshioka, M., Teshima, S.-I., 1971. The occurrence of brassicasterol in the diatoms, *Cyclotella nana* and *Nitzschia closterium*. Bull. Jpn. Soc. Sci. Fish. 37, 889–903.
Kleiven, H.K., Kissel, C., Laj, C., Ninnemann, U.S., Richter, T.O., Cortijo, E., 2008. Reduced North Atlantic deep water coeval with the glacial Lake Agassiz freshwater outburst. Science 319 (5859), 60–64.
Koç, N., Jansen, E., Haflidason, H., 1993. Paleoceanographic reconstructions of surface ocean conditions in the Greenland, Iceland and Norwegian seas through the last 14 ka based on diatoms. Quat. Sci. Rev. 12, 115–140.
Kohfeld, K.E., Fairbanks, R.G., Smith, S.L., Walsh, I.D., 1996. *Neogloboquadrina pachyderma* (sinistral coiling) as paleoceanographic tracers in polar oceans: evidence from northeast water Polynya plankton tows, sediment traps, and surface sediments. Paleoceanography 11, 679–699.
Kucera, M., et al., 2005. Reconstruction of sea-surface temperatures from assemblages of planktonic foraminifera: multi-technique approach based on geographically constrained calibration data sets and its application to glacial Atlantic and Pacific Oceans. Quat. Sci. Rev. 24 (7–9), 951–998.
Laskar, J., Robutel, P., Joutel, F., Gastineau, M., Correia, A.C.M., Levrard, B., 2004. A long-term numerical solution for the insolation quantities of the earth. Astron. Astrophys. 428 (1), 261–285.
Locarnini, R.A., Mishonov, A.V., Antonov, J.I., Boyer, T.P., Garcia, H.E., Baranova, O.K., Zweng, M.M., Johnson, D.R., 2010. World ocean Atlas 2009. In: Levitus, S. (Ed.), Temperature. NOAA Atlas NESDIS 68, vol. 1. U.S. Government Printing Office, Washington, D.C., p. 184
Lubinski, D.J., Polyak, L., Forman, S.L., 2001. Freshwater and Atlantic water inflows to the deep northern Barents and Kara seas since ca 13 14C ka: foraminifera and stable isotopes. Quat. Sci. Rev. 20 (18), 1851–1879.
Manabe, S., Stouffer, R.J., 1980. Sensitivity of a global climate model to an increase of CO2 concentration in the atmosphere. J. Geophys. Res. 85 (C10), 5529–5554.
Manno, C., Pavlov, A.K., 2014. Living planktonic foraminifera in the Fram Strait (Arctic): absence of diel vertical migration during the midnight sun. Hydrobiologia 721, 285–295.
Matthiessen, J., Baumann, K.-H., Schroeder-Ritzrau, A., Andruleit, A., Baumann, A., Jensen, S., Kohly, A., Pflaumann, U., Samtleben, C., Schäfer, P., Thiede, J., 2001. Distribution of plankton assembalbes in surface sediments of the northern North Atlantic and their relation to surface water masses. In: Schäfer, P., Ritzrau, W., Schlüter, M., Thiede, J. (Eds.), The Northern North Atlantic: A Changing Environment. Springer, Berlin, pp. 105–127.
Montero-Serrano, J.-C., Frank, N., et al., 2013. Decadal changes in the mid-depth water mass dynamic of the Northeastern Atlantic margin (Bay of Biscay). Earth Planet. Sci. Lett. 364, 134–144.
Müller, J., Massé, G., Stein, R., Belt, S.T., 2009. Variability of sea-ice conditions in the Fram Strait over the past 30,000 years. Nat. Geosci. 2 (11), 772–776.
Müller, J., Wagner, A., Fahl, K., Stein, R., Prange, M., Lohmann, G., 2011. Towards quantitative sea ice reconstructions in the northern North Atlantic: a combined biomarker and numerical modelling approach. Earth Planet. Sci. Lett. 306, 137–148.
Müller, J., Werner, K., Stein, R., Fahl, K., Moros, M., Jansen, E., 2012. Holocene cooling culminates in sea ice oscillations in Fram Strait. Quat. Sci. Rev. 47, 1–14.
Müller, J., Stein, R., 2014. High-resolution record of late glacial and deglacial sea ice changes in Fram Strait corroborates ice–ocean interactions during abrupt climate shifts. Earth Planet. Sci. Lett. 403 (0), 446–455.
Nørgaard-Pedersen, N., Mikkelsen, N., Juul Lassen, S., Kristoffersen, Y., Sheldon, E., 2007. Reduced sea ice concentrations in the Arctic Ocean during the last interglacial period revealed by sediment cores off northern Greenland. Paleoceanography 22, PA1218.
Nürnberg, D., Wollenburg, I., Dethleff, D., Eicken, H., Kassens, H., Letzig, T., Reimnitz, E., Thiede, J., 1994. Sediments in Arctic sea ice: implications for entrainment, transport and release. Mar. Geol. 119, 185–214.
Pados, T., Spielhagen, R.F., 2014. Species distribution and depth habitat of recent planktic foraminifera in Fram Strait, Arctic Ocean. Polar Res. 33, 22483.
Pflaumann, U., Duprat, J., Pujol, C., Labeyrie, L.D., 1996. SIMMAX: a modern analog technique to deduce Atlantic sea surface temperatures from planktonic Foraminifera in deep-sea sediments. Paleoceanography 11 (1), 15–35.
Pflaumann, U., et al., 2003. Glacial North Atlantic: sea surface conditions reconstructed by GLAMAP 2000. Paleoceanography 18 (3), 1065.
Pfuhl, H.A., Shackleton, N.J., 2004. Two proximal, high-resolution records of foraminiferal fragmentation and their implications for changes in dissolution. Deep-Sea Res. I 51, 809–832.
Prell, W.L., 1985. The Stability of Low Latitude Sea Surface Temperatures: An Evaluation of the CLIMAP Reconstruction with Emphasis on Positive SST Anomalies. U.S. Dept. of Energy, p. 60. Rep. TR 025.
Rabe, B., Schauer, U., Mackensen, A., Karcher, M., Hansen, E., Beszczynska-Möller, A., 2009. Freshwater components and transports in the Fram Strait - recent observations and changes since the late 1990s. Ocean Sci. 5 (3), 219–233.
Rasmussen, T.L., Thomsen, E., Slubowska, M.A., Jessen, S., Solheim, A., Koç, N., 2007. Paleoceanographic evolution of the SW Svalbard margin (76°N) since 20,000 ^{14}C yr BP. Quat. Res. 67, 100–114.
Rasmussen, T.L., Thomsen, E., Skirbekk, K., Slubowska-Woldengen, M., Klitgaard Kristensen, D., Koç, N., 2013. Spatial and temporal distribution of Holocene temperature maxima in the northern Nordic seas: interplay of Atlantic, Arctic- and polar water masses. Quat. Sci. Rev. 92, 280–291.
Reimer, P.J., et al., 2009. IntCal09 and Marine09 radiocarbon age calibration curves, 0-50,000 years cal BP. Radiocarbon 51, 1111–1150.
Risebrobakken, B., Jansen, E., Andersson, C., Mjelde, E., Hevrøy, K., 2003. A high-resolution study of Holocene paleoclimatic and paleoceanographic changes in the Nordic Seas. Paleoceanography 18 (1), 1017.
Risebrobakken, B., Dokken, T., Smedsrud, L.H., Andersson, C., Jansen, E., Moros, M., Ivanova, E., 2011. Early Holocene temperature variability in the Nordic Seas: the role of oceanic heat advection versus changes in orbital forcing. Paleoceanography 26, PA4206.
Sarnthein, M., van Krefeld, S., Erlenkeuser, H., Grootes, P.M., Kucera, M., Pflaumann, U., Schulz, M., 2003. Centennial-to-millennial-scale periodicities of Holocene climate and sediment injections off the western Barents shelf, 75°N. Boreas 32, 447–461.
Simstich, J., Sarnthein, M., Erlenkeuser, H., 2003. Paired δ18O signals of *Neogloboquadrina pachyderma* (s) and *Turborotalita quinqueloba* show thermal stratification structure in Nordic seas. Mar. Micropaleontol. 48 (1–2), 107–125.
Ślubowska, M., Koç, N., Rasmussen, T.L., Klitgaard-Kristensen, D., 2005. Changes in the flow of Atlantic water into the Arctic Ocean since the last deglaciation: evidence from the northern Svalbard continental margin, 80°N. Paleoceanography 20, PA4014.
Ślubowska, M., Rasmussen, T.L., Koç, N., Klitgaard-Kristensen, D., Nilsen, F., Solheim, A., 2007. Time-advection of Atlantic water to the western and northern Svalbard shelf since 17,500 cal yr BP. Quat. Sci. Rev. 26, 463–478.
Ślubowska, M., Koç, N., Rasmussen, T.L., Klitgaard-Kristensen, D., Hald, M., Jennings, A.E., 2008. Time-slice reconstructions of ocean circulation changes on the continental shelf in the Nordic and Barents seas during the ast 16,000 cal yr BP. Quat. Sci. Rev. 27, 1476–1492.
Spielhagen, R.F., Werner, K., Aagaard Sørensen, S., Zamelczyk, K., Kandiano, E.,

Please cite this article in press as: Werner, K., et al., Holocene sea subsurface and surface water masses in the Fram Strait – Comparisons of temperature and sea-ice reconstructions, Quaternary Science Reviews (2015), http://dx.doi.org/10.1016/j.quascirev.2015.09.007

Budéus, G., Husum, K., Marchitto, T.M., Hald, M., 2011. Enhanced modern heat transfer to the Arctic by warm Atlantic water. Science 331, 450–453.
Spielhagen, R.F., Erlenkeuser, H., 1994. Stable oxygen and carbon isotopes in planktic foraminifers from the Arctic ocean surface sediments: reflection of the low salinity surface water layer. Mar. Geol. 119, 227–250.
Stangeew, E., 2001. Distribution and Isotopic Composition of Living Planktonic Foraminifera *N. pachyderma* (Sinistral) and *T. quinqueloba* in the High Latitude North Atlantic. Ph.D. dissertation. Christian-Albrechts-University, Kiel, Germany.
Stuiver, M., Reimer, P., 1993. Extended 14C data base and revised CALIB 3.0 14C age calibration program. Radiocarbon 35, 215–230.
Ter Braak, C.J.F., Juggins, S., 1993. Weighted averaging partial least-squares regression (WA-PLS) – an improved method for reconstructing environmental variables from species assemblages. Hydrobiologia 269, 485–502.
Thornalley, D.J.R., Elderfield, H., McCave, I.N., 2009. Holocene oscillations in temperature and salinity of the surface subpolar North Atlantic. Nature 457 (7230), 711–714.
Volkman, J.K., 2006. Lipid markers for marine organic matter. In: Volkman, J.K. (Ed.), Handbook of Environmental Chemistry, vol. 2. Springer-Verlag, Berlin, Heidelberg, pp. 27–70.
Volkmann, R., 2000. Planktic foraminifer ecology and stable isotope geochemistry in the Arctic Ocean: implications from water column and sediment surface studies for quantitative reconstructions of oceanic parameters. Ber. Polarforsch. 361, 1–128.
Vinje, T., 2001. Anomalies and trends of sea-ice extent and atmospheric circulation in the Nordic seas during the period 1864–1998. J. Clim. 14, 255–267.
Wassmann, P., Peinert, R., Smetacek, V., 1991. Patterns of production and sedimentation in the boreal and polar Northeast Atlantic. In: Sakshaug, E., Hopkins, C.C.E., Øritsland, N.A. (Eds.), Proceedings of the Pro Mare Symposium on Polar Marine Ecology, Trondheim, 12-16 May 1990. Polar Research, vol. 10, pp. 209–228.
Werner, K., Spielhagen, R.F., Bauch, D., Hass, H.C., Kandiano, E., Zamelczyk, K., 2011. Atlantic water advection to the eastern Fram Strait – multiproxy evidence for late Holocene variability. Palaeogeogr. Palaeoclimatol. Palaeoecol. 308, 264–276.
Werner, K., Spielhagen, R.F., Bauch, D., Hass, H.C., Kandiano, E., 2013. Atlantic water advection to the eastern Fram Strait during the last 9 ka: multiproxy evidence for a two-phase Holocene. Paleoceanography 28, 283–295.
Werner, K., Frank, M., Teschner, C., Müller, J., Spielhagen, R.F., 2014. Neoglacial change in deep water exchange and increase of sea-ice transport through eastern Fram Strait: evidence from radiogenic isotopes. Quat. Sci. Rev. 92, 190–207.
Xiao, X., Fahl, K., Stein, R., 2013. Biomarker distributions in surface sediments from the Kara and Laptev seas (Arctic Ocean): indicators for organic-carbon sources and sea-ice coverage. Quat. Sci. Rev. 79 (1), 40–52.
Zamelczyk, K., Rasmussen, T., Husum, K., Haflidason, H., de Vernal, A., Krogh Ravna, E., Hald, M., Hillaire-Marcel, C., 2012. Paleoceanographic changes and calcium carbonate dissolution in the central Fram Strait during the last 20 ka. Quat. Res. 78, 405–416.
Zamelczyk, K., Rasmussen, T., Husum, K., Hald, M., 2013. Marine calcium carbonate preservation vs. climate change over the last two millennia in the Fram Strait: implications for planktic foraminiferal paleostudies. Mar. Micropaleontol. 98, 14–27.
Zamelczyk, K., Rasmussen, T., Husum, K., Godtliebsen, F., Hald, M., 2014. Surface water conditions and calcium carbonate preservation in the Fram Strait during marine isotope stage 2, 28.8-15.4 kyr. Paleoceanography 29, 1–12.